２００８年度

# Analysis of Cooperation Characteristics between Two Humans Based on a Musculoskeletal Model

三重大学大学院工学研究科システム工学専攻

張　楠

# Analysis of Cooperation Characteristics between Two Humans Based on a Musculoskeletal Model

**Doctoral Dissertation**

June 2008

*Submitted in partial fulfillment of the requirements for*
***Doctor of Philosophy Degree***
*in Mechanical Engineering*

By

**Nan ZHANG**

*System Engineering Division, Graduate School of Engineering*
*Mie University, Japan*

Supervisor
Professor Ryojun IKEURA

# ACKNOWLEDGEMENT

First of all, I would like to extend my heartfelt gratefulness to all those who gave me the possibility to finish this dissertation.

Especially I am obliged to Prof. Kazuki Mizutani who provided me with the chance to make studies and carry out research work in System Design laboratory of Mie University.

I am deeply indebted to my supervisor Prof. Ryojun Ikeura whose patient guidance, valuable hints, and stimulating encouragement helped me in all the time of studying and researching. Just because of him, I made progress in different stages of this research work, which finally enabled me to complete my Ph.D. courses. I would like to give my sincerest gratitude and honor to him.

I am most grateful to the committee of professors who reviewed this dissertation thoroughly over the last phase of my Ph.D. program. To follow their comments, I made the perfection of this dissertation possible, which eventually bring satisfactory completion of my Ph.D. courses. My true thankfulness is due to them.

I am bound to say that without the help from Lab. Assistant Hideki Sawai, I might

spend much time on setting up the experimental system. His enthusiastic teaching and constructive advice enriched my knowledge about how to use the experimental equipment, which made it easy for me to get ahead with my experiments. I would like to show my deepest appreciation to him.

I want to thank Dr. Kato and my lab mates for their kind helps and hearty friendliness. My lab mate Ph.D. student Mr. Yuanxin Wang was of great help in my difficult times, I have furthermore to thank him for all his help and interest in this research work. I also want to thank graduate student Mr. Kazunori Nishio for all his assistance on this research work. Besides, I want to thank my lab mate Ph.D. student Mr. Mizanoor Rahman for his looking closely at my several papers in English, correcting mistakes and offering suggestions for improvement.

Last of all, I would like to express my special thanks to my family members and friends whose endless love and support enabled me to accomplish this research work.

# CONTENTS

# CHAPTER 1

# INTRODUCTION

## 1.1 Robot History

The word robot derived from the Czech noun robota meaning labor was an accomplishment of the Czech cubist painter and writer Josef Capek. This frequently used word first appeared in the play "R.U.R (Rossum's Universal Robots)" (1921) by the Czech writer Karel Capek. Robot entered the English language in 1923. The word robotics first appeared in the short science fiction story "Runaround" (1942) by the Russian-born American writer Isaac Asimov[1].

According to the Robot Institute of America (1979), the definition of a robot is[2]:
a reprogrammable, multifunctional manipulator designed to move materials, parts, tools, or specialized devices through various programmed motions for the performance of a variety of tasks.

According to the Webster dictionary (1993), the definition of a robot is[2]:
An automatic device that performs functions normally ascribed to humans or a machine in the form of a human.

One of the first robots was the clepsydra or water clock, which was made in 250 B.C. Ever since robots have been invented, humans have been very interested in

them. With the continuous progress and increasing demand of the society, robot science has been developing rapidly. Till now, robotic technology has made many things possible, such as (1) the productivity improvement in industry, (2) the exploration in the outer space or the deep sea, (3) the delicate medical operation, (4) the dangerous missions for the military and police, (5) the new types of entertainment, and (6) the life-like new toys able to talk and respond like real creatures.

## 1.2 Background

As shown in Fig. 1.1, most of the contemporary robots that combine high speed and high accuracy play a vital role in performing relatively simple and repetitive tasks in industry. They are the ways and means for further productivity improvements. However, the robots for improving productivity in industry have gotten dissatisfied with the needs of the aging society of the 21st Century.

Fig. 1.1 A robot for productivity improvement in industry.

Today Japan is a country with the world longest life expectancy of 80 years, and it is expected to become an extremely "aged society", in which about a quarter of the people are aged. This aging society may be characterized by a shortage of the productive population first of all. In the face of the aged society of the 21st century, the development of human machine interface technology that responds to such a lack of labor force will be indispensable. The society is calling upon the world to propose innovative design ideas that will help realize new interfaces for human functions. In order to cope with these present-day social challenges, robot technologies, which are taking on the role of enhancing and performing the functions of life forms—particularly humans—are viewed as a potential composite technology leading to effective solutions to the aging society. As a matter of fact, in the 1990s, some manufacturers have already turned their attention to developing medical and health care devices, targeting the rapidly aging society, or produced entertainment robots, to accommodate changes in society's values about work and living. These robots represent a new paradigm of human–robot symbiosis.

### 1.2.1 Human–Robot Cooperation

Historically, in order to avoid industrial accidents, there has been a separation between workers and robots in industrial settings. However, with the continuously increasing labor-shorted problems in the aging society, we have been expecting an improvement in control technology—the improvement to make a potential for human to work with robots safely. In such a human-robot interface, as shown in Fig. 1.2[9]-[14],

robots are supposed to work in collaboration with human by performing smooth movements. The cooperative robots can perform various cooperative tasks with humans, for example, in hospitals they can help nurses to carry patients, and so on. As we know, to a certain extent, in order to accomplish cooperative tasks with human, robots have to possess human characteristics inevitably.

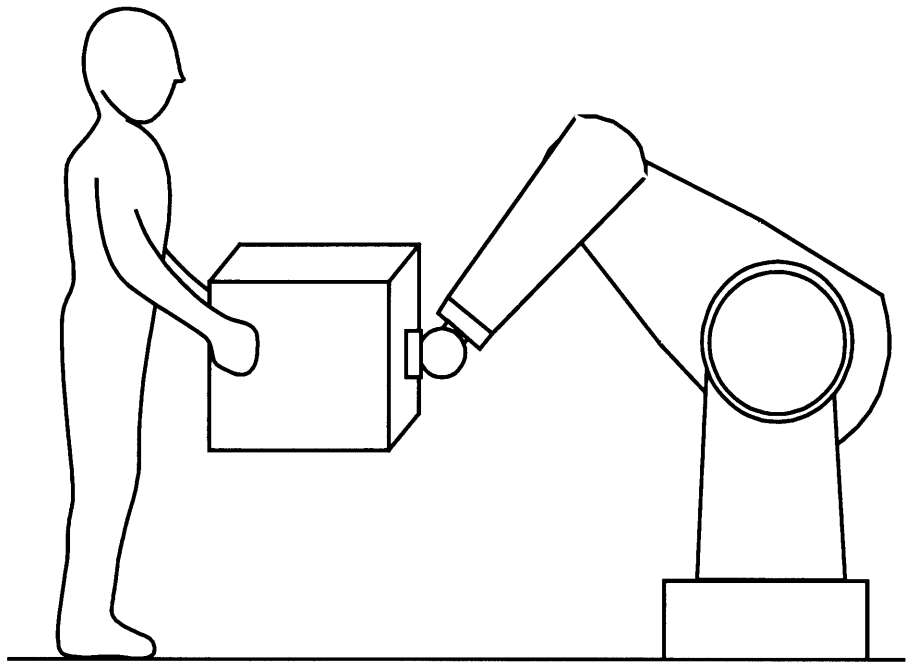

Fig. 1.2 A human-robot cooperative task.

Till now many researchers have tried to propose control methods for multiple cooperative robots to work in human–robot cooperation[3]-[6]. Some other control methods for robots cooperating with humans have been developed[7],[8], however the truth is, we found that they were proposed without considering human characteristics.

We expect a human–robot symbiosis, in which it will be natural to see cooperation between humans and robots in both simple and complex tasks. To realize the cooperation with humans, robots are supposed to be human-friendly and to be designed with human characteristics.

Ikeura *et al.* made some studies on cooperative control for a robot[13]-[17]. In these studies by examining the human characteristics in a cooperative task between two humans, he found that the human performance could be expressed by impedance control. Then he applied the impedance parameters found in the experiment to a robot performing cooperative task with a human, and he found best performance between the human and the robot. Furthermore, he proposed a variable impedance model after investigating human characteristics in a human–human cooperative task[9]-[12]. Analyzing this model provided the impedance characteristics, based on which a variable impedance control method was developed for human–robot cooperation.

Besides, Rahman *et al.* investigated a one degree-of-freedom human–human cooperative task by examining the horizontal movement of an object, as shown in

Fig. 1.3[18]-[20]. In this experiment, a linear motor served as an actuator to drive the slider; the two human subjects kept their forearms horizontally while moving the handles on the slider cooperatively, and the correlation between acceleration and force was analyzed. Two major types of cooperation were detected: master–slave and master–master. They observed that in master–slave cooperation the master moved the object, while the slave only held the object and performed passive movements. From this, they proposed that master–slave cooperation was more appropriate for human–robot cooperation, with the human acting as the master and the robot as the slave. The slave's characteristics could then be applied to the design of the robot's control system. Further, they determined the impedance characteristics of the slave's arm, and implemented the estimated parameters to control robots performing tasks in cooperation with a human[21]. They observed that, in executing human–robot cooperative tasks, the proposed control method resulted in good interaction between the robot and its human partner. This study convinced us that the human arm characteristics that Rahman *et al.* identified can be applied to the control systems involving robots working cooperatively with humans.

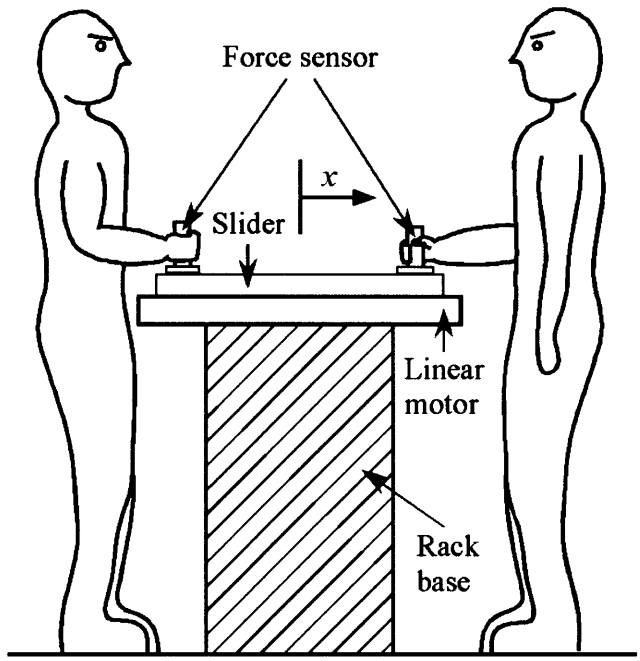


Fig. 1.3 Human–human cooperative task that requires moving an object horizontally.

## 1.3 Research Objective

As mentioned above, Rahman *et al.* analyzed the impedance characteristics of the human forearm[22],[23]. The author's purpose was to further their work by building and analyzing a biomechanical model of the human arm based on the musculoskeletal system around the elbow. The author used this model to determine the characteristics of the human arm that was reported to be one of the most complex articulations in the human body[24] during execution of human–human cooperative tasks.

Some theories of the characteristics of the human arm based on the musculoskeletal structure have been proposed. For example, Gomi *et al.* has found that a human not only accelerates the arm but also changes its impedance characteristics by activating specific muscles[25]. Moreover, he has shown that the stiffness and viscoelasticity of the human multi-joint arm change under different contraction conditions during posture maintenance and the task of regulating force[26]. These theories help the author understand the spatial characteristics of the human arm. It has been pointed out that a motor command from the central nervous system regulates a variable structure of the impedance characteristics. But at the same time, the author understands that these commands are not concerned with human–robot cooperative characteristics and are inapplicable to robotic control. This study is aimed at understanding the characteristics of the human arm that apply to robotic control in human–robot cooperative tasks.

Typically, as shown in Fig. 1.4, the human arm performs motions in tasks with

multiple degrees-of-freedom. Many researchers have attempted studies based on a multiple degree-of-freedom model of the human arm. Unfortunately, it proved very difficult to obtain quantitative estimations because they could not extract the correct parameters. To simplify the problem, the author considered a model of cooperative motion between two humans in a dynamic system with a single-rotational degree-of-freedom (1-DOF). This allows a much simpler dynamic analysis of the human arm characteristics. Investigations based on a biomechanical model of the human arm in such a dynamic system have been performed (the investigations have mostly been based on idealized physical representations of the musculoskeletal system[27]). The author gets to know that in terms of modeling muscle action, some muscles have very broad attachments, while others are divided into several bundles attached to different bones. These can be modeled by dividing the muscles into several lines of action. The choice of lines must be made based on both anatomical and mechanical considerations. To this end, for dynamic simulation of the complex musculoskeletal system, the author developed a mass-spring-damper-friction biomechanical model based on the musculoskeletal system around the elbow[27]-[29].

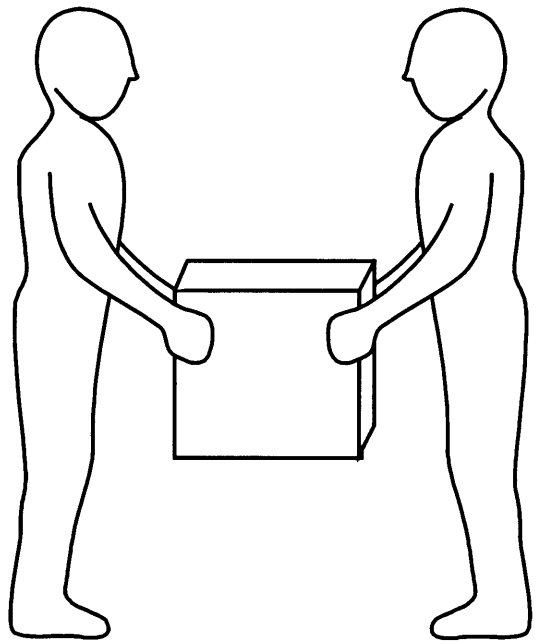

Fig. 1.4 A human–human carry task.

Rahman *et al.* defined master–slave and master–master cooperations in their study without any reference to the musculoskeletal system around the elbow. In this study, the author investigates the human arm characteristics based on the musculoskeletal system around the elbow in both the master–slave cooperative motion and the master–master cooperative motion. Although the parameters or characteristics estimated in the experiments cannot be directly implemented in robotic control, the author assumed that better cooperative characteristics may be achieved if the human arm characteristics found in this study are implemented in human–robot cooperative tasks by taking advantage of the experimental method that Rahman *et al.* proposed.

# CHAPTER 2

# HUMAN ARM MODELING

In the aging society, cooperative robots are expected to be designed human-friendly with safe and reliable service capacity for human. In other words, based on different final service object, it is essential for such intelligent robots to possess human characteristics of different parts. This means that before designing, we have to know well about the human characteristics. In this study, first of all, the author needed to attain a better understanding about the human arm.

## 2.1 Human Arm

The human body is incredibly versatile, its structure is light and the human organism operates with an incredible efficiency. Among the movable parts of the human body, the upper limbs are used most frequently. The main function of the upper limb is grasp and manipulation. This is also used as a walking aid to support the body during gait.

### 2.1.1 Human Arm Musculoskeletal System

In human anatomy, the upper limb (also upper extremity) is the region of the shoulder to the fingertips. The upper limb includes the shoulder, arm (upper arm,

elbow and forearm), wrist and hand. Among the above structures of the upper limb, in this section, the author only introduces the arm shown in Fig. 2.1. And Fig. 2.2 is the simplified image of the arm.

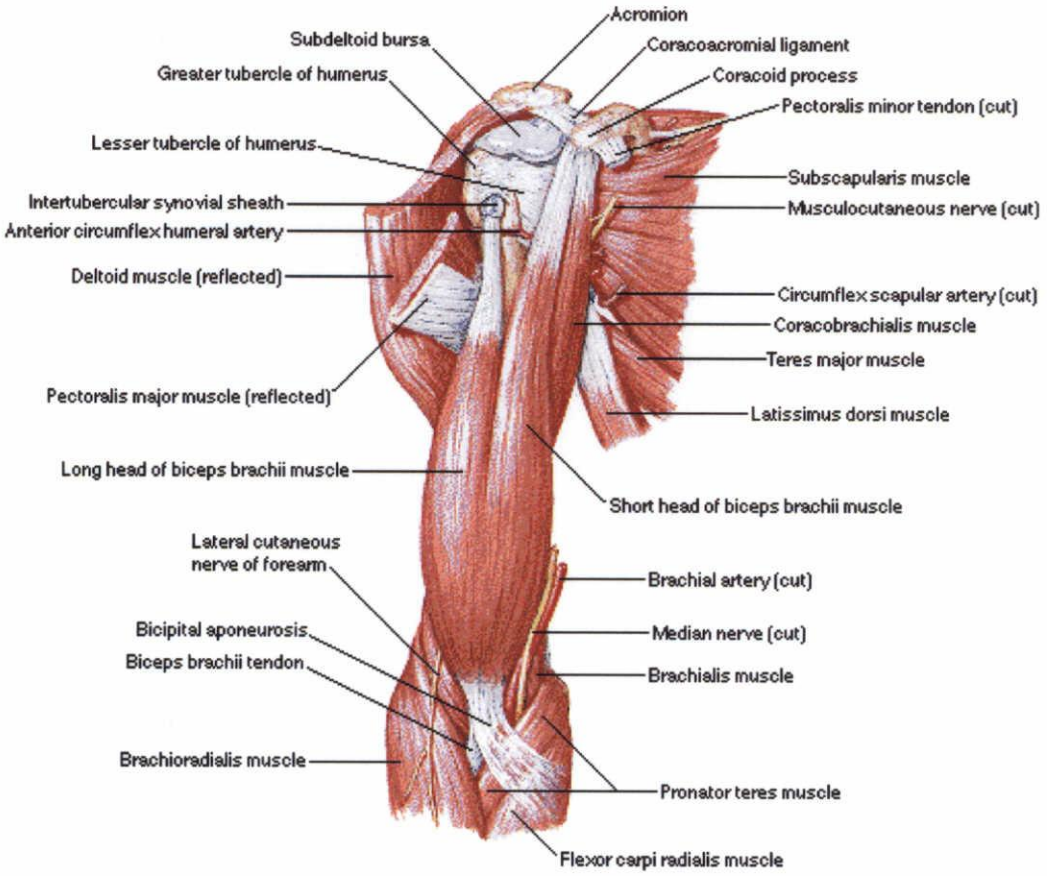


Fig. 2.1 Human arm musculoskeletal system.

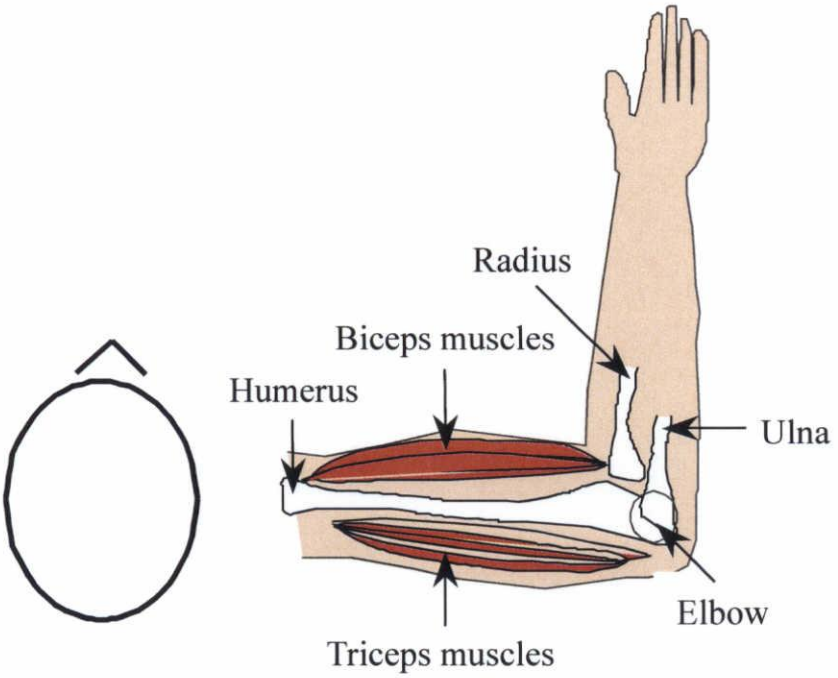


Fig. 2.2 Simplified image of the human arm musculoskeletal

The arm is made up of three long bones[30]: the humerus in the upper arm and the ulna and radius in the forearm arm. The prominent long arm bone representing the upper arm is the humerus. It is attached to the scapula, or shoulder blade, at its ball-shaped end, which rests in the shallow cup called the glenoid fossa located in the scapula. Its other end meets the radius, as well as the ulna at the elbow, with which it forms a hinge that allows the arm to straighten and bend. The upper arm and forearm are connected at the elbow by the hinge joint between the humerus and ulna. The radius and ulna are linked at the elbow in a way that allows human to rotate the hand and forearm by more than 180 degrees. The ulna bone forms the point of the elbow.

The shoulder and arm bones have roughened patches on their surfaces where muscles are attached[31],[32]. The main function of the upper arm muscles is flexion and extension of the elbow joint. A secondary function of this muscle group is pronation and supination of the arm. The upper arm is separated into the muscle groupings of the biceps and triceps.

The biceps group comprises four muscles that flex the arm at the elbow joint[33]: the biceps brachii, brachialis, brachioradialis and pronator teres. The biceps muscle (Biceps Brachii) is a two-headed muscle with point of origin under the deltoid and point of insertion just below the elbow, it is located on the front of the humerus and permits lifting the arm and bending the elbow when it contracts, as well as rotation of the forearm and pronation (downward twist) of the wrist. The tapered ends of the biceps muscle are firmly attached by strong tendons to the periosteum of the skeleton.

The upper end of the muscle is attached to the scapula by two tendons and the lower end is attached to the radius of the forearm. The radius is moved upwards as the biceps muscle contracts. The biceps muscle is connected to the bone by the biceps tendon—the proximal biceps tendon at the shoulder joint (scapula) and the distal biceps tendon at the elbow (radius).

The triceps group consists of two muscles[33]: the triceps brachii and anconeus. The triceps muscle (Triceps Brachii) is a large three-headed muscle that is located at the back of the upper arm and attaches to the portion of the ulna called the olecranon. The three heads of the triceps muscle include: the long head, lateral head and medial head. The long head that originates on the border of the shoulder blade is attached to the inner part of the scapula. The lateral head that originates on the outside of the humerus and the medial head that originates on the back of the humerus are attached to the humerus, or the main upper arm bone. The primary function of each is to extend the forearm and straighten the elbow. Each head originates in a different place but comes together at a single tendon that attaches to the back of the ulna at the olecranon process. The triceps muscle is attached to the bone by the triceps tendon, which inserts into the back of the elbow. It works opposition to the biceps muscle with permitting straightening the arm and elbow when it contracts, as well as supination (upward twist) of the wrist. The radial nerve travels down the arm and supplies movement to the triceps muscle.

The elbow joint is a ginglymus—an example of a hinge joint, or a joint that

moves in only one direction[34]. It is formed by three bones: the humerus of the upper arm and the paired radius and ulna of the forearm. Articulations between the trochlea of the humerus with the ulna and the capitulum of the humerus with the head of the radius comprise the joint. The bony prominence at the very tip of the elbow is the olecranon process of the ulna. Ligaments are present in the elbow joint. The major ligaments are the ulna collateral ligament, radial collateral ligament and annular ligament. These ligaments provide strength and support to the joint, as do the surrounding muscles. The ulna collateral ligament is a strong fan-shaped condensation of the fibrous joint capsule. It is located on the medial side of the joint, extending from the medial epicondyle of the humerus to the proximal portion of the ulna. This ligament prevents excessive abduction of the elbow joint. Two main movements are possible with the elbow joint, the hinge-like bending and straightening of the elbow (flexion and extension) happens at the articulation (joint) between the humerus and ulna, as well as the complex action of turning the forearm over (pronation or supination) happens at the articulation between the radius and ulna.

## 2.2 Human Arm Biomechanical Model

We know that, as the muscles never work in isolation, natural movements always involve the motions of all the bones. Thus, for a complete analysis, it is important to consider the motion of the mechanism as a whole[27]. Once the anatomy and biomechanics of the musculoskeletal system have been observed, qualitative

descriptions and classifications can serve as a basis for parameter definitions. These are necessary for a theoretical mechanical analysis of the system, which generally leads to its quantitative description.

After examining the musculoskeletal system around the elbow shown in Fig. 2.2, the author developed a human arm biomechanical model that includes the biomechanical properties required for proper dynamic analysis. The model is shown by Fig. 2.3. The whole body remains fixed, except for the arm. The structure consisting of the biceps and the triceps muscles is considered mechanically analogous to a mass-spring-damper-friction model, the forearm is considered a rigid body, and the elbow a joint. In this model, $I_h$, $c$, $k$, $f_f$, $u_B$, and $u_T$ are the parameters of the human arm biomechanical model—inertia, damping factor, stiffness, friction, strength of the biceps muscles, and strength of the triceps muscles, respectively. Note that $c$, $k$, and $f_f$ vary with the strength exerted by the arm, $\theta$ is the angular displacement of the forearm, $f_B$ is the force generated by the biceps muscles, $f_T$ is the force generated by the triceps muscles, and $\tau_E$ is the external torque exerted on the arm.

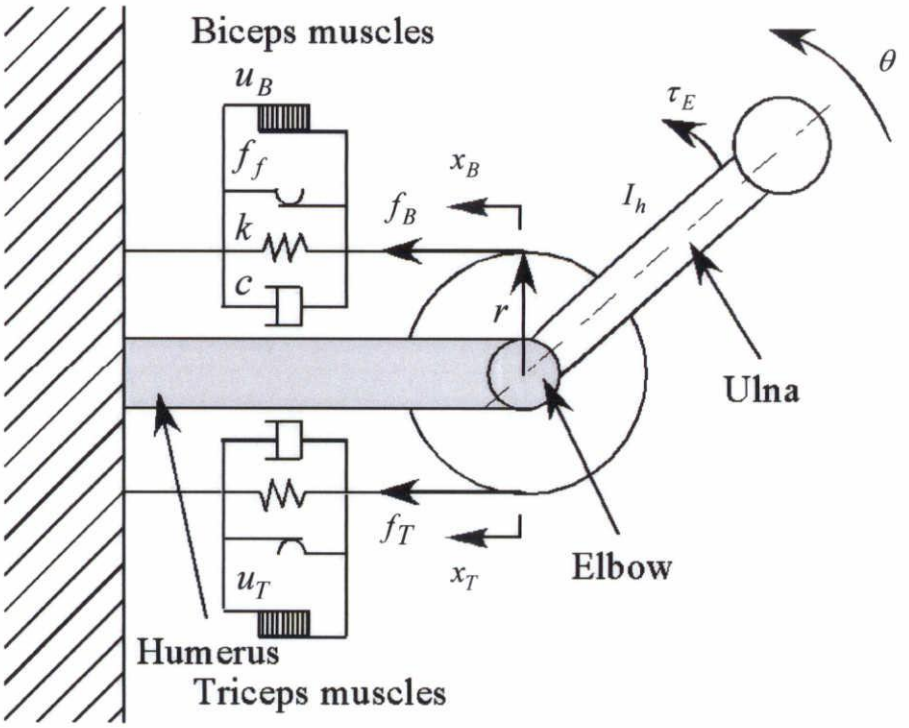


Fig. 2.3 Human arm biomechanical model.

Given this biomechanical model, the equation of motion for the arm (the relationship among the inertia torque of the forearm, the torques generated by the biceps and triceps muscles, and the external torque) can be expressed as:

$$I_h\ddot{\theta} = \tau_B - \tau_T + \tau_E \tag{1}$$

The parameters for the biceps and triceps muscles have the following relationship:

$$f_B = -f_f \cdot \mathrm{sgn}(\dot{x}_B) - kx_B - c\dot{x}_B + u_B \tag{2}$$

$$f_T = -f_f \cdot \mathrm{sgn}(\dot{x}_T) - kx_T - c\dot{x}_T + u_T \tag{3}$$

and the angular displacement that the forearm moves and the displacements happened because of the movement of the biceps and triceps muscles have the following relationship:

$$\mathrm{sgn}(\dot{x}) = \begin{cases} 1 & (\dot{x} > 0) \\ -1 & (\dot{x} < 0) \end{cases}$$

$$x_B = r\theta$$

$$x_T = -r\theta$$

Then Eqs. (2) and (3) can be expressed as:

$$\tau_B = -\tau_f \cdot \mathrm{sgn}(\dot{\theta}) - kr^2\theta - cr^2\dot{\theta} + u_B r \tag{4}$$

$$\tau_T = \tau_f \cdot \mathrm{sgn}(\dot{\theta}) + kr^2\theta + cr^2\dot{\theta} + u_T r \tag{5}$$

Substituting Eqs. (4) and (5) into Eq. (1), the author obtains the following equation:

$$I_h\ddot{\theta} + 2cr^2\dot{\theta} + 2kr^2\theta + 2\tau_f \cdot \mathrm{sgn}(\dot{\theta}) = (u_B - u_T)r + \tau_E \tag{6}$$

From Eq. (6), the author obtains the second-order differential equation of motion:

$$I_h\ddot{\theta} + C\dot{\theta} + K\theta + \tau_F = (u_B - u_T)r + \tau_E \quad (7)$$

where $C = 2cr^2$, $K = 2kr^2$, and $\tau_F = 2\tau_f \cdot \mathrm{sgn}(\dot{\theta})$.

## 2.3 Rotational 1-DOF Experimental System

Rahman *et al.* determined master–master and master–slave cooperations in translational 1-DOF motion[18]. In this study, on the basis of the above-mentioned human arm biomechanical model, the author focuses on the characteristics of the human arm in rotational 1-DOF master–master and master–slave cooperative motions. This single rotational degree-of-freedom experimental system is pictured by Fig. 2.4.

Fig. 2.4 Image of rotational 1-DOF experimental system.

Depicted by Fig. 2.5, this rotational 1-DOF experimental system provides both master–slave and master–master cooperative motion. In this model, the master (involved in master–slave and master–master cooperation) is the one who performs active arm movements throughout the motion, the slave (involved in master–slave cooperation) performs passive arm movements by keeping the arm muscles completely relaxed during the motion, and the semi-master (involved in master–master cooperation) switches roles from slave to master on the halfway point of the motion. The master and slave/semi-master humans lay their right forearms on the respective armloads and perform rotation with their elbow joints as the rotation centers. Their forearms move synchronously as a result of the timing belt. As shown in Fig. 2.5, $I$ is the moment of inertia of the load, $\theta$ is the angular displacement of the forearm, and $\tau_1$ and $\tau_2$ are the torques exerted by the arms on the armloads. In the figure, the plus sign that appears on the display represents the angular displacement signal of the forearm, and the square is the simulated sine wave signal serving as a target position. Both signals are sent to the display monitors from the controller computer. When performing master–slave cooperative motion, throughout the motion, the master human watches the display monitor to track the target position—the correct track is determined by fitting the plus sign into the square sign, and the slave human performs passive arm movement without looking at the display monitor. When performing master–master cooperative motion, the master human tracks the motion on the display monitor during the motion. Meanwhile, the semi-

master human does not look at the display monitor when playing the role of slave from the beginning to the halfway of the motion, but when switching to play the role of master from the halfway point of the motion, this human starts to watch the display monitor to track the motion like master. That is why this human is called semi-master in this study.

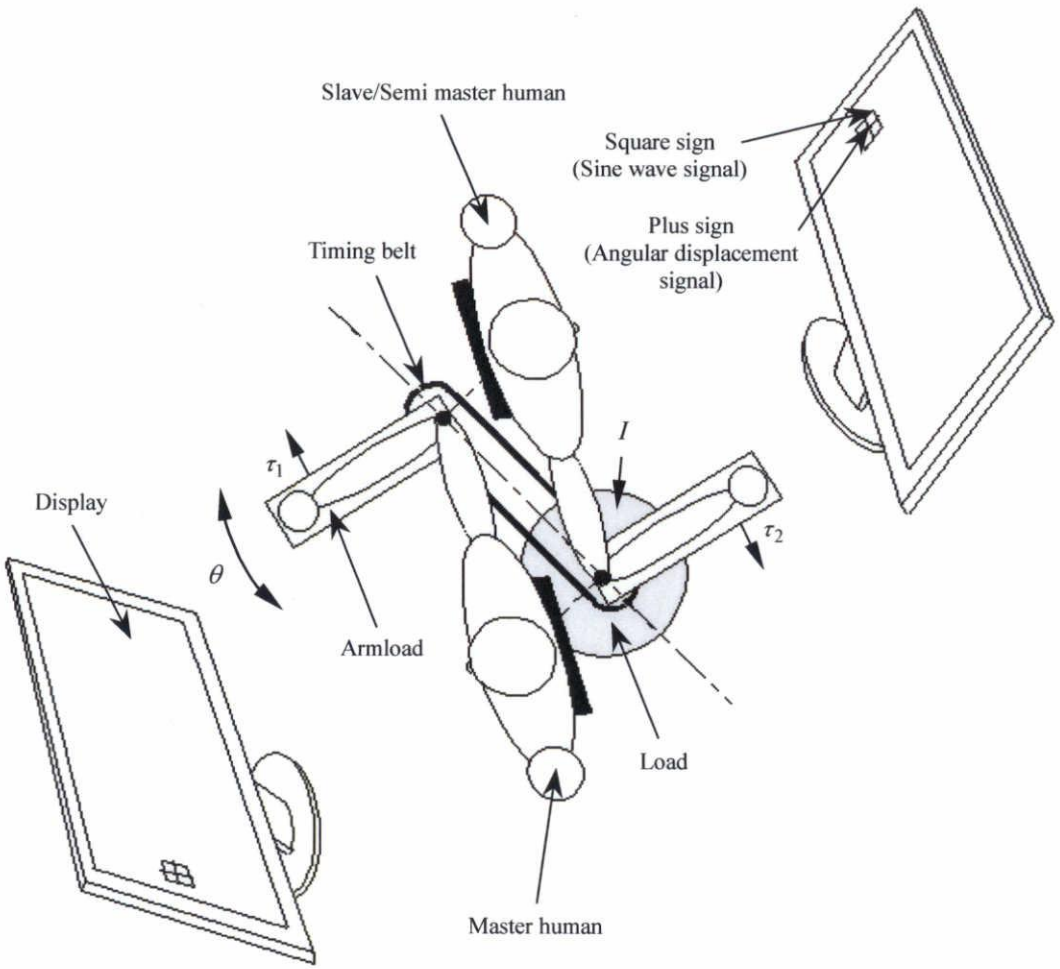


Fig. 2.5 Model of rotational 1-DOF cooperative motion.

For this rotational 1-DOF dynamic system, the equation of motion can be expressed as:

$$I\ddot{\theta} = \tau_1 + \tau_2 \tag{8}$$

By introducing $\alpha$ $(0 \le \alpha \le 1)$ as the distribution ratio of the inertia torque, $I\ddot{\theta}$, $\tau_1$, and $\tau_2$ can be expressed as:

$$\tau_1 = \alpha I\ddot{\theta} + \tau_{\text{int}} \tag{9}$$

$$\tau_2 = (1-\alpha)I\ddot{\theta} - \tau_{\text{int}} \tag{10}$$

where $\tau_{\text{int}}$ is the internal torque generated between the two humans during the motion.

In the previous paragraphs, the author has given a literal explanation for the master–master and master–slave cooperation. Here, the author wants to give a quantitative explanation for them by using the equations.

Rahman *et al.* experimentally defined two types of cooperation depending on the value of $\alpha$ [18]. One is master–master cooperation where $\alpha \neq 1$, in which the torques for the masters can be expressed by Eqs. (9) and (10). The second is master–slave cooperation where $\alpha = 1$, in which the torques, denoted as $\tau_M$ for the master and as $\tau_S$ for the slave, can be expressed as follows:

$$\tau_M = I\ddot{\theta} + \tau_{\text{int}} \tag{11}$$

$$\tau_S = -\tau_{\text{int}} \tag{12}$$

Eqs. (9) and (10) show that in master–master cooperation, both master humans must control both the inertia and internal torque. Eqs. (11) and (12), however, show that, in

master–slave cooperation, the master human controls both the inertia and internal torque, while the slave human controls only the internal torque. Therefore, Rahman *et al.* proposed that the slave characteristics should be applied to robotic controller design; in this case, the controller is only needed to control the internal torque, thus simplifying the controller design. Thus, the author considered it necessary to investigate the characteristics of the human arm in master–slave cooperative motion.

With regard to evaluation of sensation, the above equations show that in master–master cooperation, the master humans share the load to make the task easier for both. In master–slave cooperation, however, the master human has to carry the entire load. Thus, the author considered that it makes sense to investigate the characteristics of the human arm in master–master cooperative motion.

# CHAPTER 3

# EXPERIMENTAL SYSTEM AND PRELIMINARY EXPERIMENTS

## 3.1 Experimental System

As shown in Fig. 3.1, the experimental system consists primarily of the synchronous torque system, the armloads, and the measurement system. The synchronous torque system transmits the torque between the two armloads via a timing belt fixed onto the two armload shafts. A preliminary tension test proves that during rotation, there is hardly any transmission delay between the two armloads, and that the friction caused is minimal. The armload supports the subject's arm (forearm). Each armload is fitted with rubber for isolation and comfort. Both the synchronous torque system and the armloads have high rigidity but generate low inertia torque. The load can be attached to or detached from the synchronous torque system. The measurement system consists of the cam position sensor, with the cam fixed to the shaft of the armload, and two force sensors fixed between the armloads and the arms connected to the shafts of the armloads. To measure the angular displacement of the forearm, the cam and eddy current sensor are used to obtain a signal proportional to the angular displacement. To measure the torque acting on the

armload from the forearm, the force sensor and dynamic strain amplifier are used to obtain a signal proportional to the torque. Both the angular displacement signal from the eddy current sensor and the torque signal from the dynamic strain amplifier are converted from analog to digital by an A/D board interfaced to the controller computer, where the signals are used for data processing. The angular displacement is shown as a plus on the display monitor; the simulated sine wave signal is shown as a square, which provides the target position for the master/semi-master human to track to perform active arm movement.

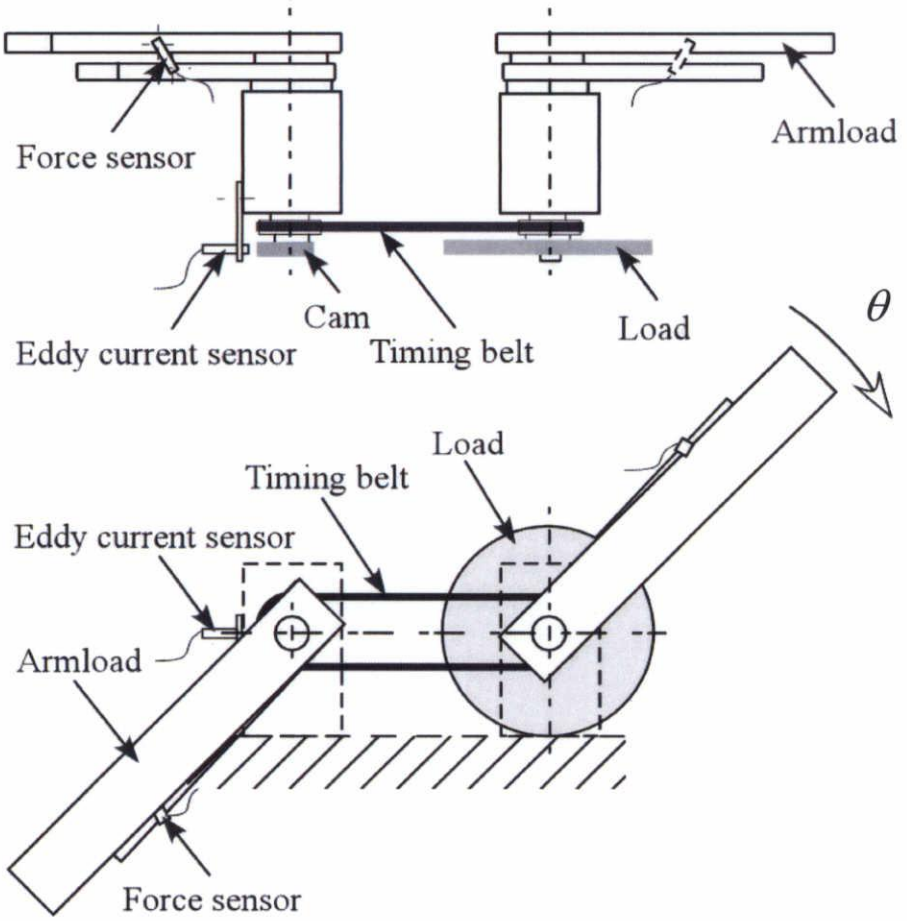


Fig. 3.1 Experimental system.

Figure 3.2 shows a brief illustration of the experimental measurement method. The torques measured by force sensors 1 and 2, along with the angular displacement measured by the eddy current sensor, are inputted to the controller computer through the A/D board. The sampling time is 0.004 s. The angular displacement and simulated sine wave are outputted to the display monitors. To avoid the experimental data being affected by noise, a filter with a cut-off frequency of 6.95 Hz is used.

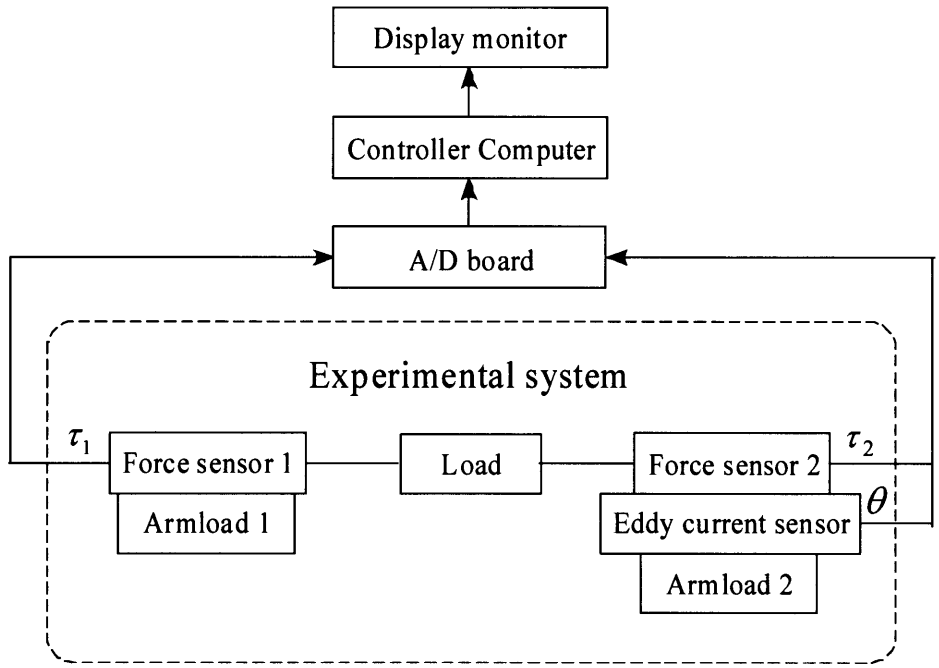


Fig. 3.2 Schematic diagram of the measurement method.

## 3.2 Preliminary Experiments with a Slave

Eight right-handed, healthy subjects consisting of six men, aged 22, 23, 36, and 52 years, and two women, aged 25 and 35 years, participated in the experiments.

Prior to the experiments on cooperative motion, the author performed three preliminary experiments to get an idea of the characteristics of the slave's arm. The eight subjects were instructed to play the role of the slave. As shown in Fig. 2.5, each of these subjects put the right forearm on the armload, keeping the elbow joint (i.e. the rotation center of the forearm) coaxial with the axis of the armload. The subject was seated in an armchair, motionless and comfortable. The height of the armchair was adjusted to keep the armload at the subject's chest level. During the motion, the subject performed passive arm movement—keeping the arm muscles completely relaxed and not looking at the display monitor.

Before the first preliminary experiment, a heavy load ($I$ = 0.527 kg·m$^2$) was attached to the experimental system. Then, the author observed the step response of the subject's relaxed arm; its input was the external torque for stretching or contracting the arm, and the time behavior of its output was the angular displacement shown in Fig. 3.3. The arm (settled on the armload) was stretched by an external torque (0.4 N·m) exerted in a clockwise (CW) direction. Once the torque became stable, the arm was released. The arm shook and finally reached a stationary state at a maximum CW equilibrium position, where the angular displacement was zero. Similarly, the arm was contracted using the same magnitude of external torque but

exerted in the counterclockwise (CCW) direction. Again, the arm was released after the torque became stable. The arm shook and finally reached a stationary state at a maximum CCW equilibrium position, where the angular displacement measured was 0.33 rad. As shown in Fig. 3.3, there are maximum equilibrium positions[35]-[37] in the CW and CCW directions. It was observed that, if a different initial state was given, the arm could stop anywhere between the two maximum equilibrium positions. By the way, the equilibrium position defined in this study is where the relaxed arm is in a stationary state so that the external torque (as $\tau_E$ shown in Eq. (7)) is zero. Through such step responses, the author realizes that the slave's arm experienced both a restoring effect and static friction, and dynamic friction might also exist. This illustrates that in developing a biomechanical model of the human arm for human–robot cooperation, a mass-spring-damper-friction model would be more appropriate than the mass-spring-damper model traditionally suggested.

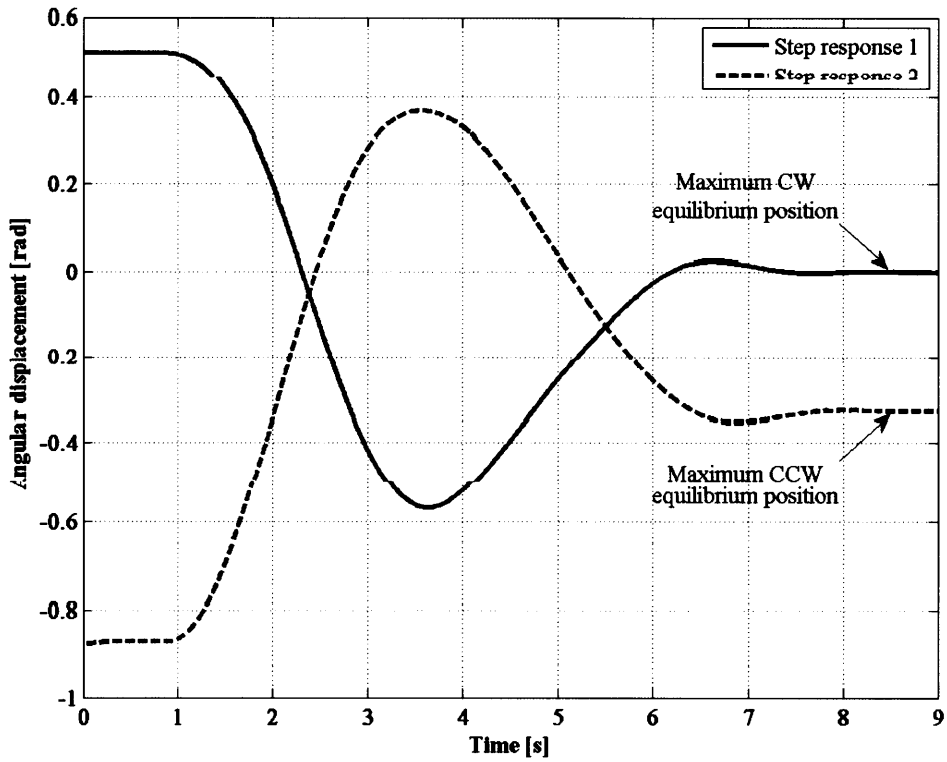


Fig. 3.3 Step response of subject A.

In the second preliminary experiment, the author observed the stiffness and friction characteristics of the subject's relaxed arm, as shown in Fig. 3.4. The arm was moved to a position where the upper arm and the forearm were nearly straight; this position was named $A_{CW1}$. The measurement began here. At a very low speed, the arm was moved CCW toward the body to a position as close as possible to the chest; this position was named $A_{CCW1}$. Without a break, the arm was then moved CW to position $A_{CW1}$, completing a round-trip motion. Similarly, the arm was continuously moved CCW to position $A_{CCW2}$ ($A_{CCW2} < A_{CCW1}$), and then moved CW to position $A_{CW2}$ ($A_{CW2} < A_{CW1}$). These round-trip motions were performed nonstop four times. In Fig. 3.4, the horizontal and vertical axes represent angular displacement and torque, respectively. In the CW direction, the slope of the curve decreases gradually from position $A_{CCW1}$, and is then constant as the arm nears position $A_{CW1}$. As soon as the direction changes to CCW at position $A_{CW1}$, the slope of the curve becomes very steep (90 degrees) momentarily, then decreases for a while, and then becomes constant again (same as the constant slope in the CW direction) within the range of $R_S$ shown in Fig. 3.4. Note that the gap between the curves for the CW and CCW directions remains almost invariable only within the range of $R_S$. Because the speed of the arm movement is so low, the angular acceleration $\ddot{\theta}$ and angular velocity $\dot{\theta}$ can be deemed to be zero. Moreover, considering the slave role that the subject played, $u_B$ and $u_T$ in Eq. (7) are both zero, due to the relaxation of the biceps and the triceps muscles. Therefore, the measured torque (acting on the armload) in Eq.

(7) consists of the restoring and friction torques. Thus, the author thinks that the slope of the curve indicates the stiffness, *K*, and the gap between the curves indicates the dynamic friction of the slave's arm. It was observed that, the torque increased momentarily right after the direction changed, although the arm remained still. This seemed to be responsible for the static friction torque. When the arm started to move, static friction was replaced by dynamic friction, which increased gradually and was then constant within the range of $R_S$.

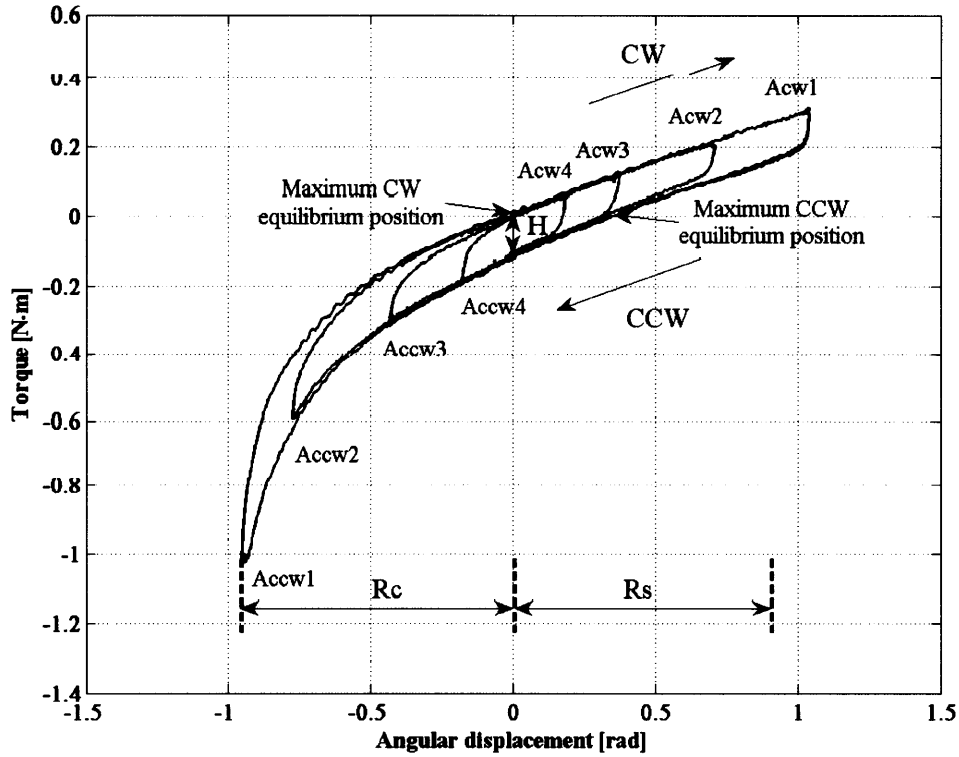


Fig. 3.4 Stiffness and friction characteristics of subject A.

In order to verify again the result from the second preliminary experiment, the author carried out another preliminary experiment. The arm was moved very slowly to complete four-time round-trip motions as shown in Fig. 3.5. The movements were like those in the second preliminary experiment, but were only within the range of $R_S$ shown in Fig. 3.4. It is shown in Fig. 3.5 that the slope of the curves for both the CW and CCW is about constant, and the gap between the curves is almost invariable. Thus, these convince the author again that within the range of $R_S$, the slope of the curve indicates the stiffness $K$, and the gap between the curves indicates the dynamic friction of the slave's arm. It was also observed that, among the eight subjects, the thicker the subject's arm was, the greater the stiffness and dynamic friction were. Table 3.1 shows the average parameters for the slope and the gap (denoted by $H$) within the range of $R_S$ for the eight subjects. For subject A, it was found that the angle between the maximum CW and maximum CCW equilibrium positions in Figs. 3.3 and 3.4 was 0.33 rad. For all the eight subjects, it was observed that, the angle between the maximum CW equilibrium position and the shoulder was nearly $1.4 \pm 0.08$ rad.

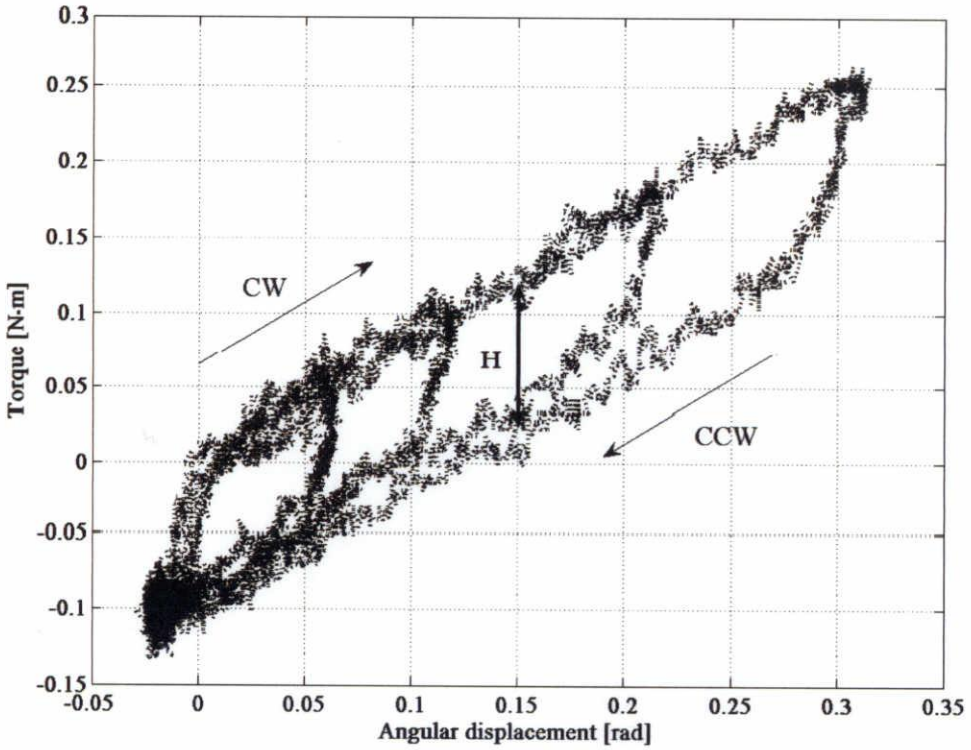


Fig. 3.5 Stiffness and friction characteristics of subject G, within range of $R_S$.

Table 3.1 Average parameter of slave's arm within range of $R_S$.

| Female/Male | A (M) | B (F) | C (F) | D (M) | E (M) | F (M) | G (M) | H (M) |
|---|---|---|---|---|---|---|---|---|
| Age | 22 | 35 | 25 | 23 | 22 | 36 | 23 | 52 |
| Slope (N·m/rad) | 0.35 | 0.45 | 0.55 | 0.57 | 0.68 | 0.93 | 1 | 1.3 |
| Gap *H* (N·m) | 0.12 | 0.13 | 0.19 | 0.20 | 0.21 | 0.24 | 0.26 | 0.56 |

On the basis of these characteristics, the author began the investigation of the human arm characteristics within the range of $R_S$. It is also thought that humans typically perform arm movements within this range. In this study, the cooperative motions were all performed within the range of $R_S$.

# CHAPTER 4

# MASTER-SLAVE COOPERATIVE EXPERIMENTS

## 4.1 Master-Slave Cooperative Motion

In the following experiments, every possible pair combination of the eight subjects was considered (16 pair combinations altogether). Each pair of subjects was instructed to perform the master–slave cooperative motion by playing the roles of both the master and the slave. Throughout the motion, the master subject performed active arm movements while watching the display monitor to keep on track, while the slave subject performed passive arm movement, by keeping the arm muscles completely relaxed and not looking at the display monitor.

### 4.1.1 Slow Cooperative Motion

In this experiment, each pair of subjects was instructed to perform master–slave cooperative motion at a low speed. The average angular velocity was approximately 0.07 rad/s. The motion was not in one direction, but was a round trip, with the go path in the CW direction opposite the body, and the return path in the CCW direction.

The characteristics of the slow cooperative motion are shown in Fig. 4.1 by three

separate graphs. In the upper graph, the horizontal and vertical axes represent time and angular velocity, respectively. In the middle graph, the horizontal axis represents time and the vertical axis represents the angular displacement and torque for the slave. In the lower graph, the horizontal and vertical axes represent the angular displacement and torque for the slave. In the upper graph, the angular velocities at points A, B, C, and D, as well as at points P, Q, R, and S are almost same. This means that within this time, the inertia torque $I\ddot{\theta}$ can be deemed to be zero, and the damping torque $C\dot{\theta}$ to be constant. Moreover, in the lower graph it is possible to connect points A, B, C, and D as well as points P, Q, R, and S to form two straight, parallel lines. The gap between the two lines is almost invariable. According to Eq. (7), for the slave's arm, the stiffness $K$, indicated by the slope, is almost constant, and the torque, indicated by $H$, which may include the dynamic friction torque $\tau_F$ and the damping torque $C\dot{\theta}$, is almost constant too.

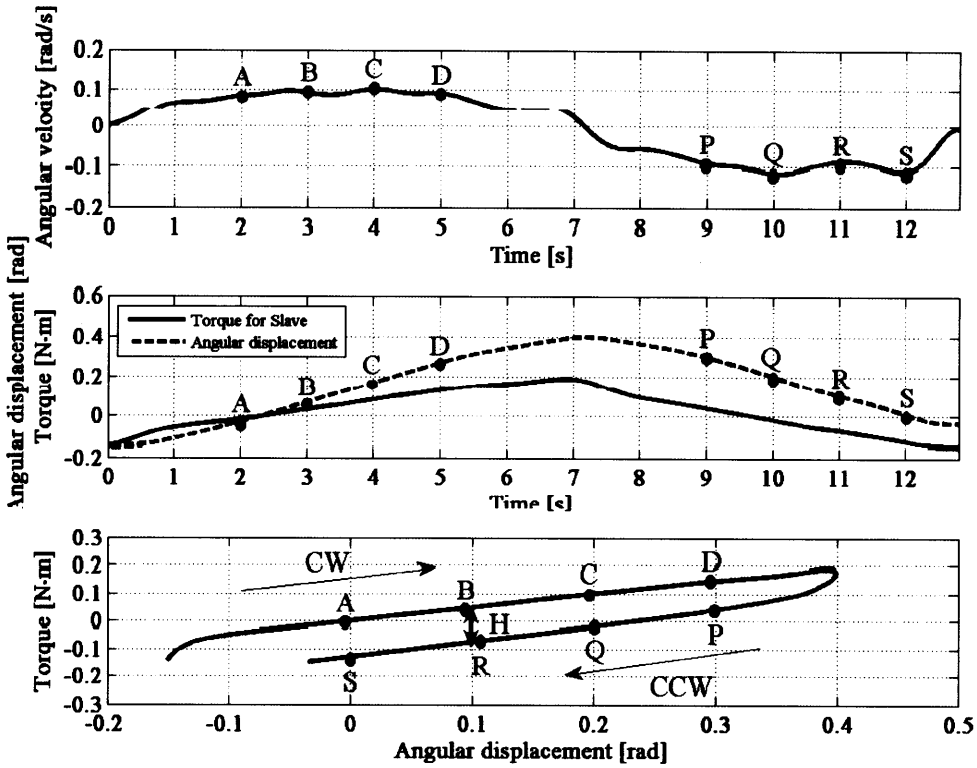


Fig. 4.1 Slow cooperative motion performed by subject C as master and subject B as slave.

In addition to Fig. 4.1, Figs. 4.2 to 4.14 show the characteristics of the slow cooperative motion performed by other pair combinations.

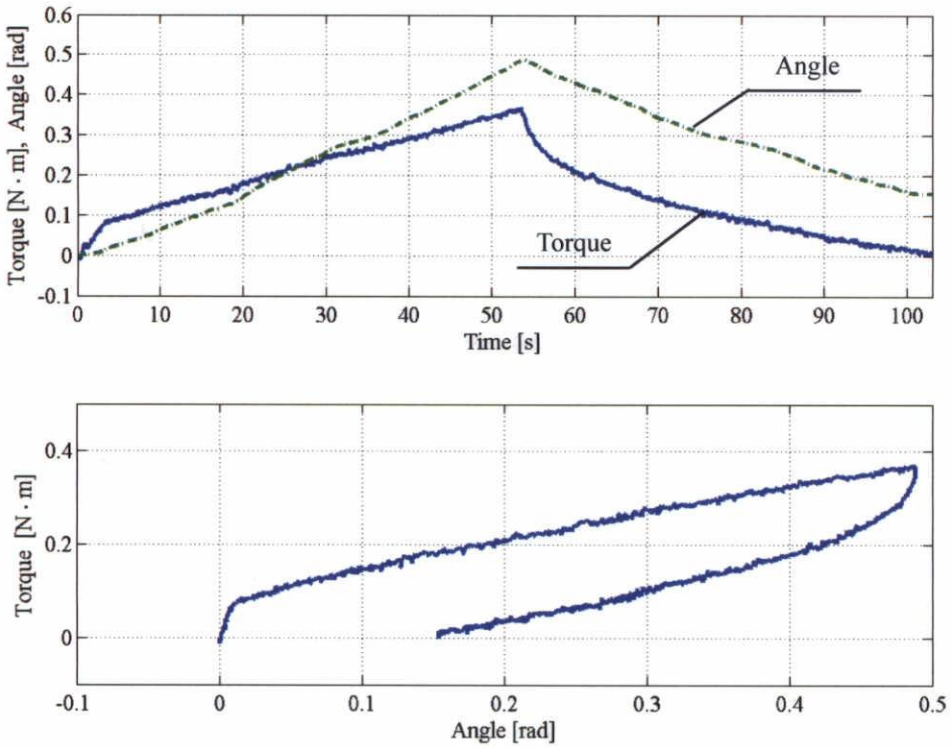


Fig. 4.2 Slow cooperative motion performed by subject A as master and subject B as slave, within 103 sec.

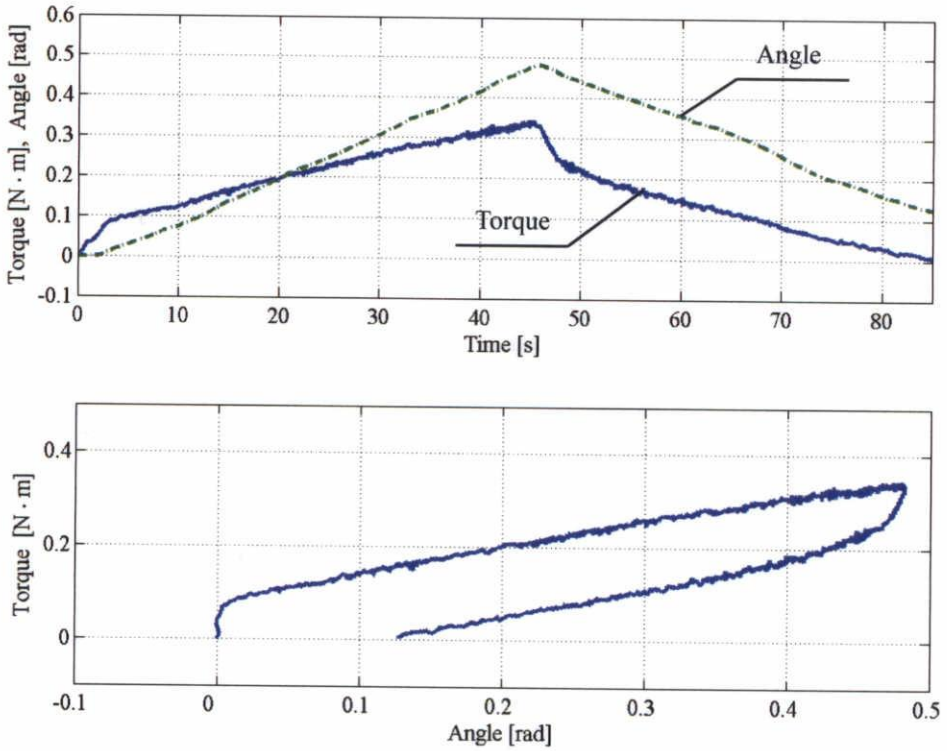


Fig. 4.3 Slow cooperative motion performed by subject D as master and subject B as slave, within 85 sec.

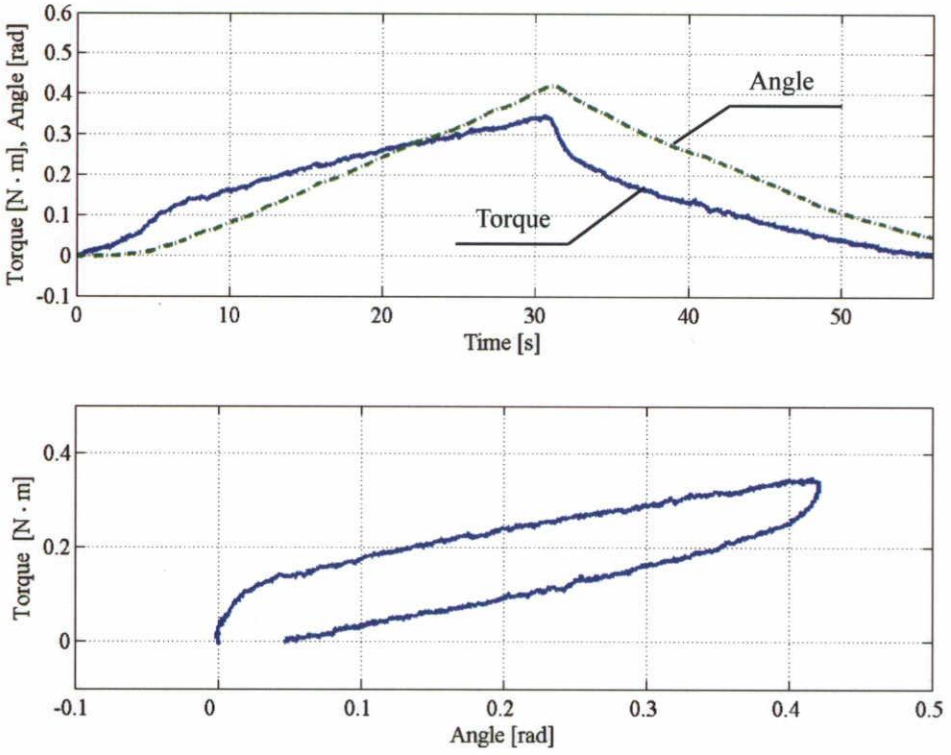


Fig. 4.4 Slow cooperative motion performed by subject E as master and subject B as slave, within 56 sec.

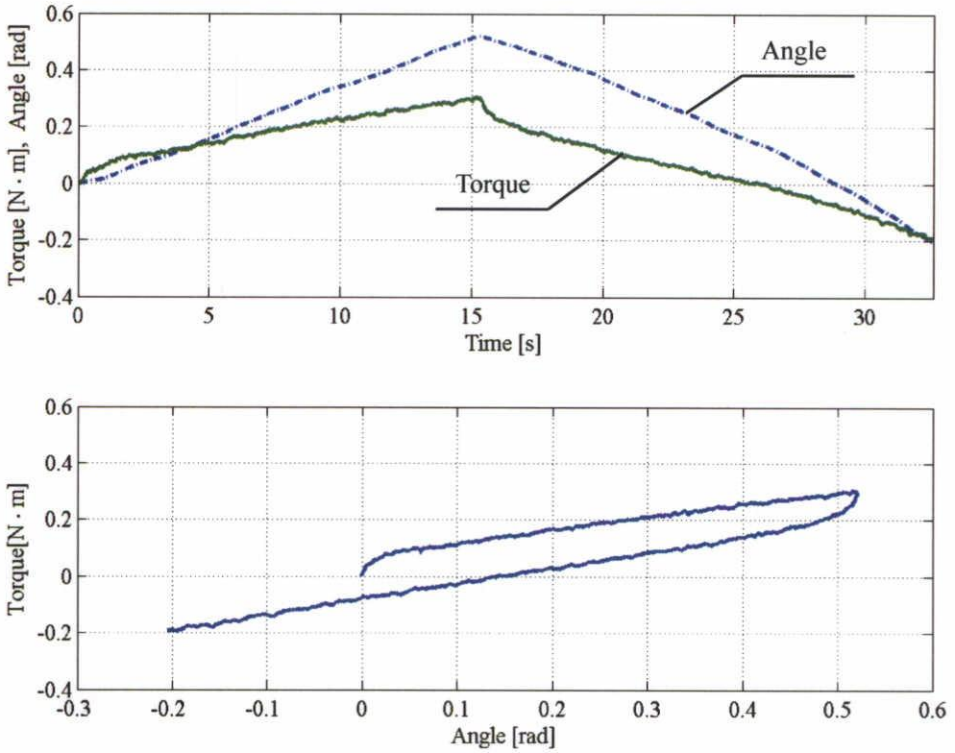


Fig. 4.5 Slow cooperative motion performed by subject F as master and subject B as slave, within 33 sec.

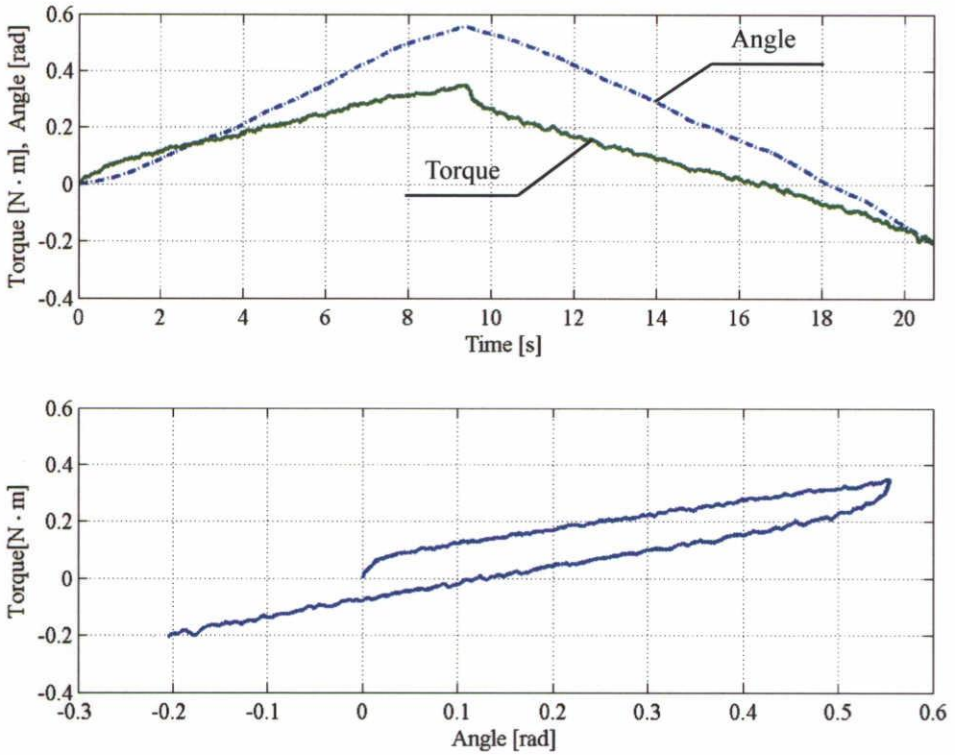


Fig. 4.6 Slow cooperative motion performed by subject G as master and subject B as slave, within 21 sec.

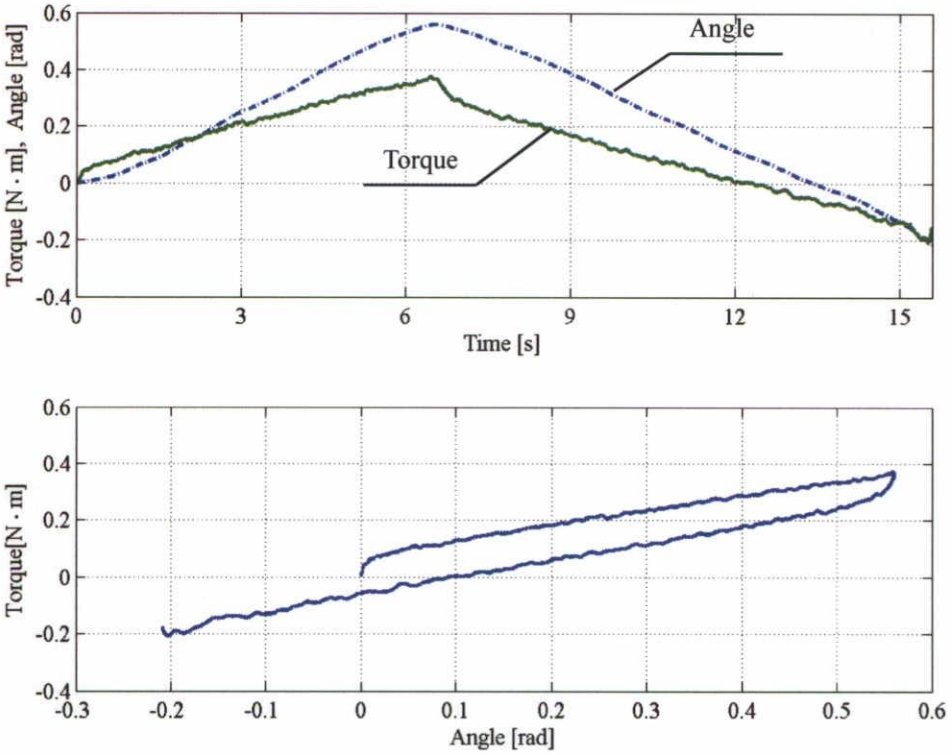


Fig. 4.7 Slow cooperative motion performed by subject H as master and subject B as slave, within 15.5 sec.

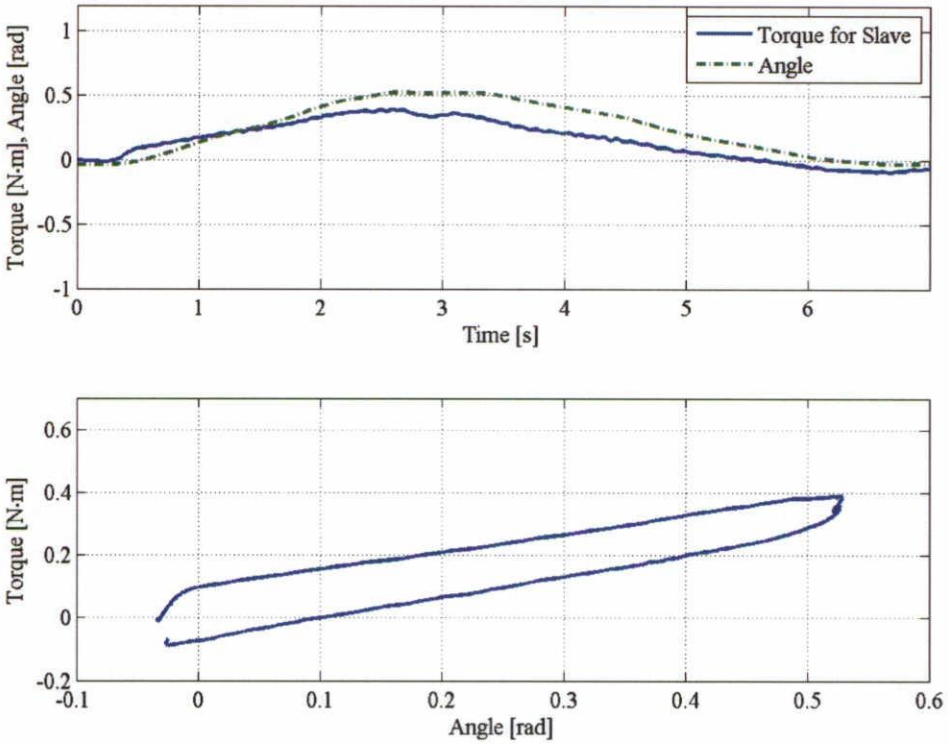


Fig. 4.8 Slow cooperative motion performed by subject A as master and subject C as slave, within 7 sec.

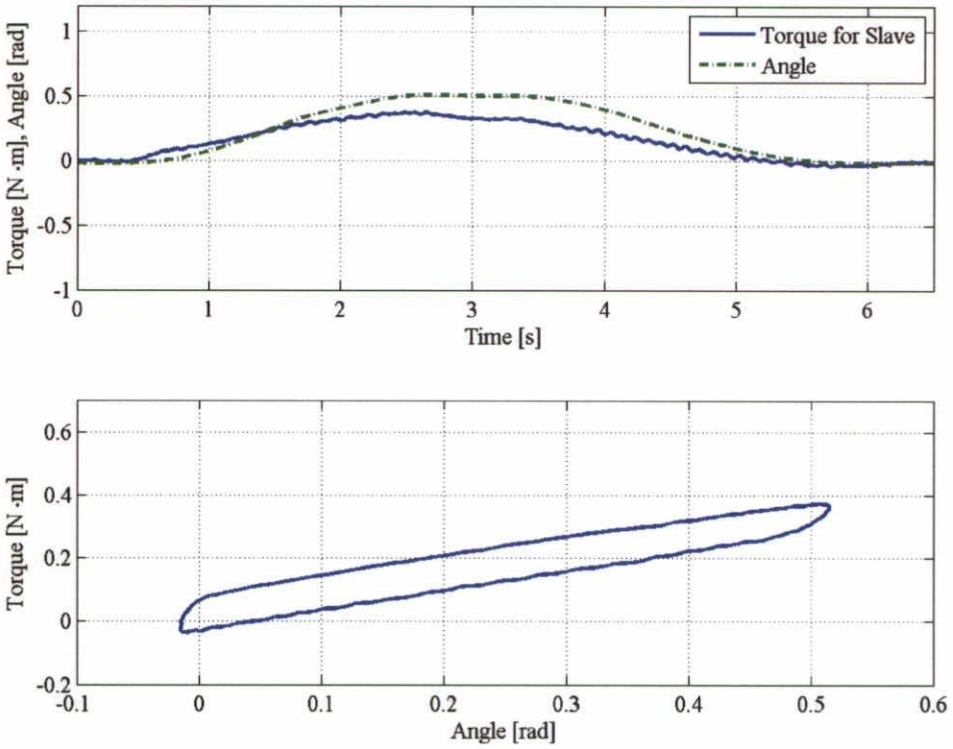


Fig. 4.9 Slow cooperative motion performed by subject B as master and subject C as slave, within 6.5 sec.

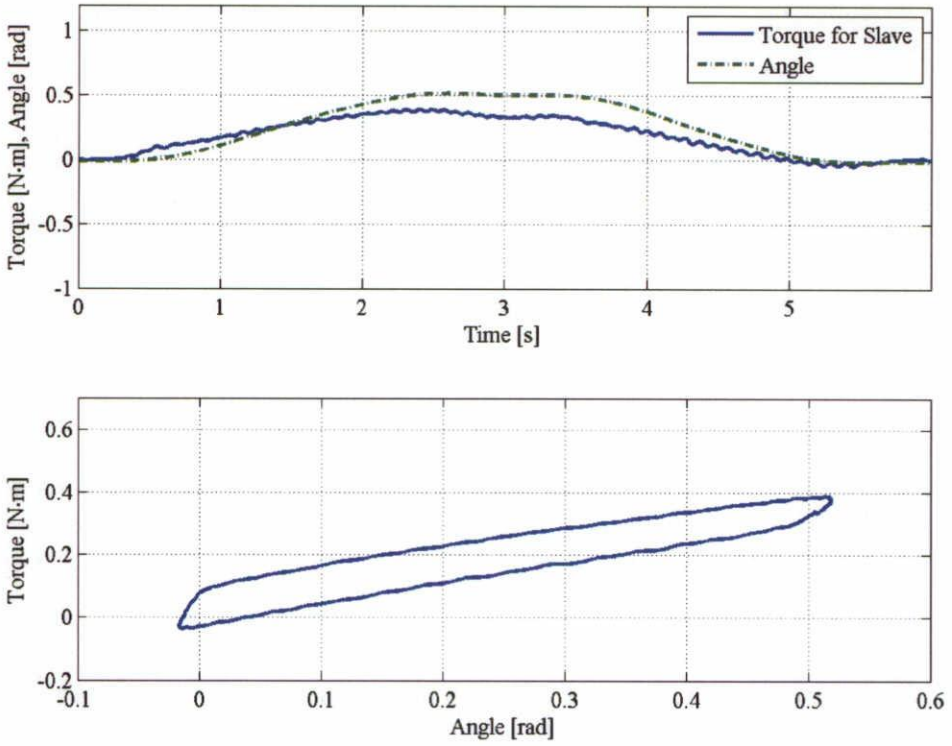


Fig. 4.10 Slow cooperative motion performed by subject D as master and subject C as slave, within 6 sec.

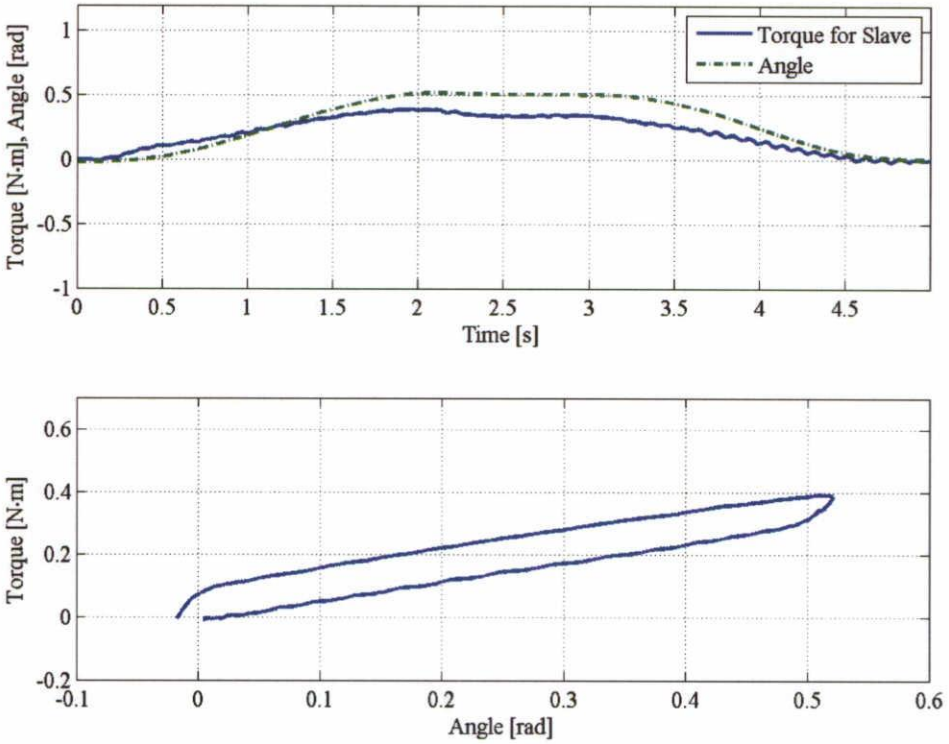


Fig. 4.11 Slow cooperative motion performed by subject E as master and subject C as slave, within 5 sec.

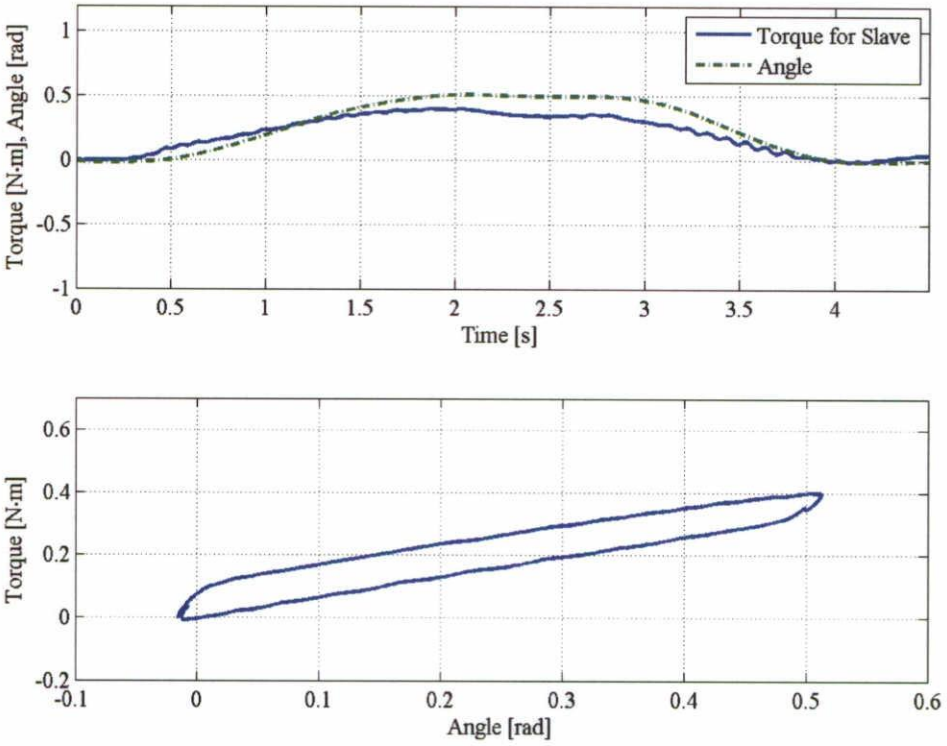


Fig. 4.12 Slow cooperative motion performed by subject F as master and subject C as slave, within 4.5 sec.

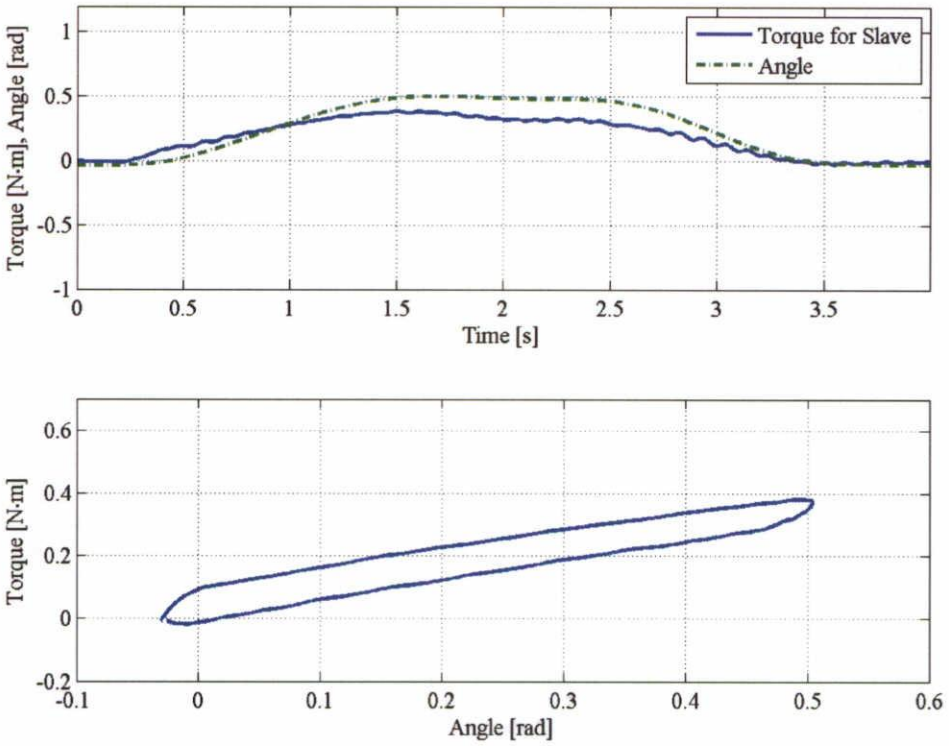


Fig. 4.13 Slow cooperative motion performed by subject G as master and subject C as slave, within 4 sec.

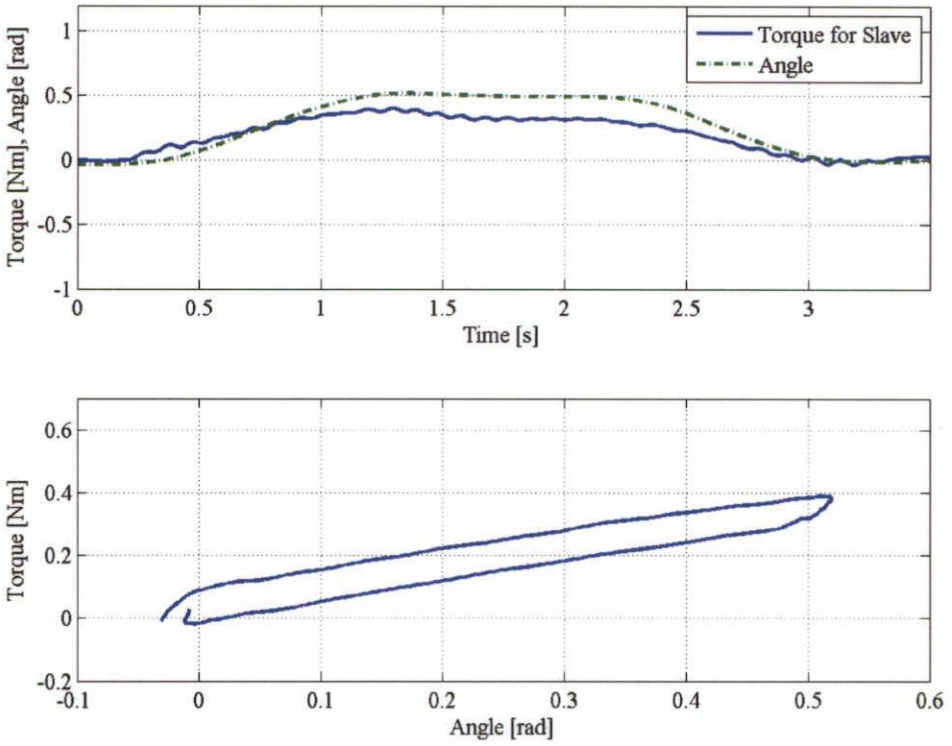


Fig. 4.14 Slow cooperative motion performed by subject H as master and subject C as slave, within 3.5 sec.

### 4.1.2 Quick Cooperative Motion

In this experiment, each pair of subjects was instructed to perform master–slave cooperative motion in one round trip at a high speed. The average angular velocity was approximately 0.6 rad/s.

The characteristics of the quick cooperative motion are shown in Fig. 4.15. The torque shown in the graphs is obtained by subtracting the arm's inertia torque from the torque exerted by the arm on the armload. According to Eq. (7), for the master, this torque can be expressed as $\tau_E - I_h\ddot{\theta} = C\dot{\theta} + K\theta + \tau_F + (u_T - u_B)r$, and for the slave as $\tau_E - I_h\ddot{\theta} = C\dot{\theta} + K\theta + \tau_F$. In the upper graph, the angular velocities at points A, B, C, and D, as well as at points P, Q, R, and S are almost the same, indicating that within this time, the inertia torque $I\ddot{\theta}$ can be deemed to be zero and the damping torque $C\dot{\theta}$ to be constant. In the lower graph, the curves have almost the same shape in either the slope or the value of $H$ as those in Fig. 4.1. In fact, the speed of motion in Fig. 4.15 is much higher than that in Fig. 4.1. Thus, the author thinks that if the angular velocity-dependent damping torque $C\dot{\theta}$ exists, the two lines in both CW and CCW direction shown in Fig. 4.15 would not be straight, and the value of $H$ should also be different. This tells the author that for the slave's arm, its parameter is unrelated to the speed of the motion—the damping factor $C$ is zero—and the stiffness $K$ as well as the dynamic friction torque $\tau_F$ are almost constant.

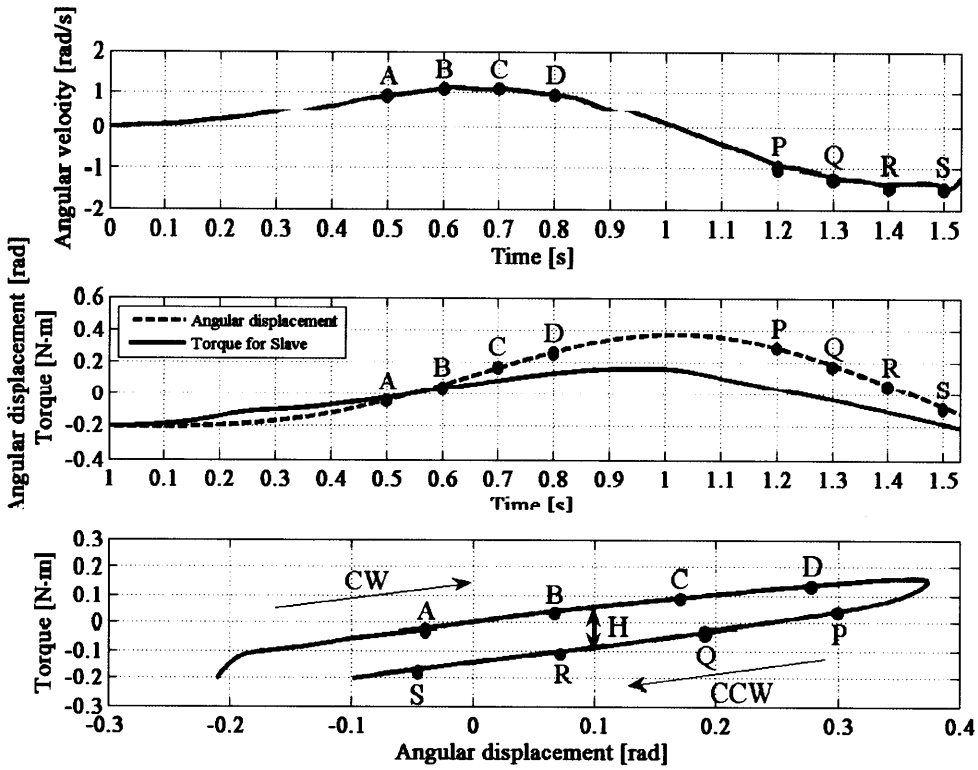


Fig. 4.15 Quick cooperative motion performed by subject F as master and subject B as slave.

In addition to Fig. 4.15, Figs. 4.16 to 4.21 show the characteristics of the quick cooperative motion performed by other pair combinations.

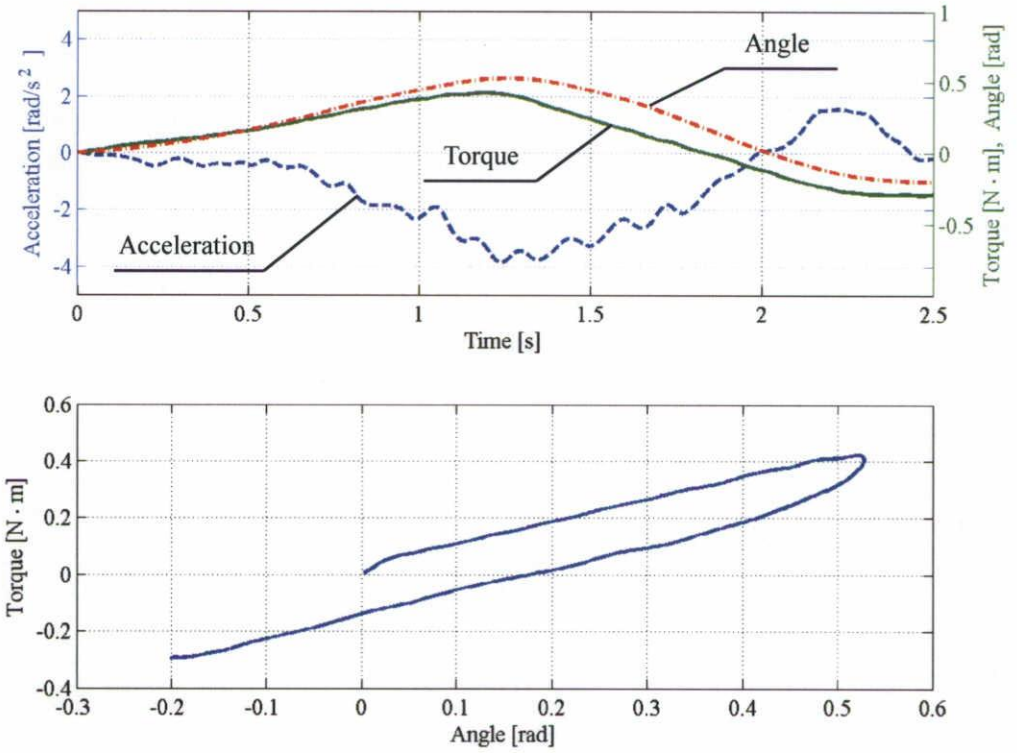


Fig. 4.16 Quick cooperative motion performed by subject A as master and subject B as slave, within 2.5 sec.

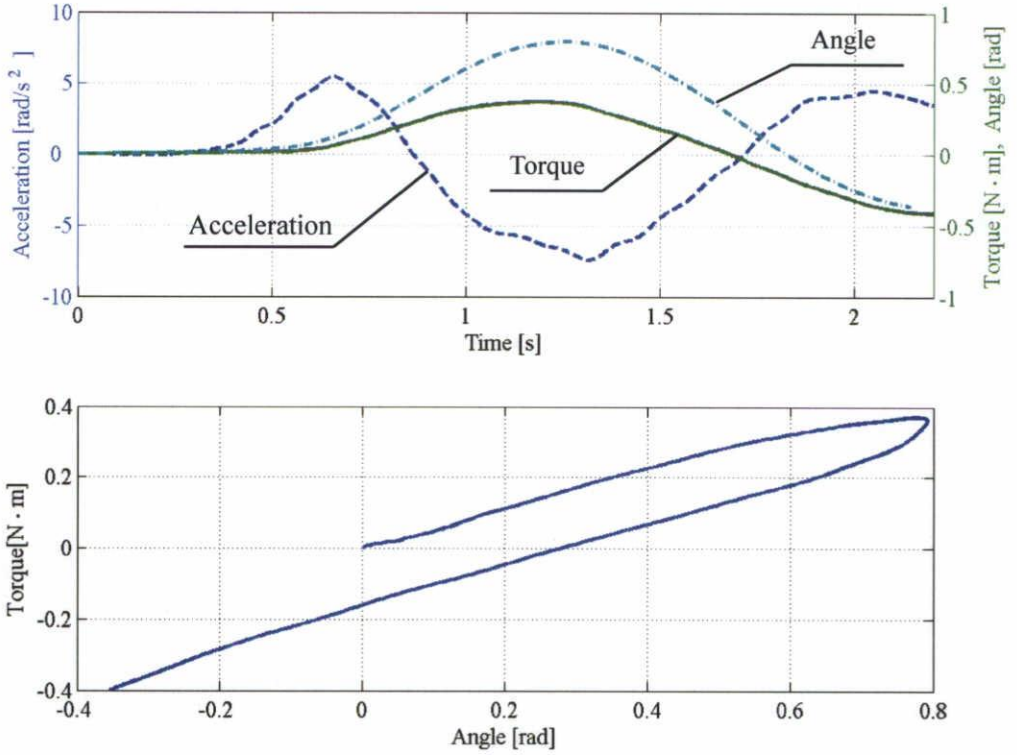


Fig. 4.17 Quick cooperative motion performed by subject C as master and subject B as slave, within 2.2 sec.

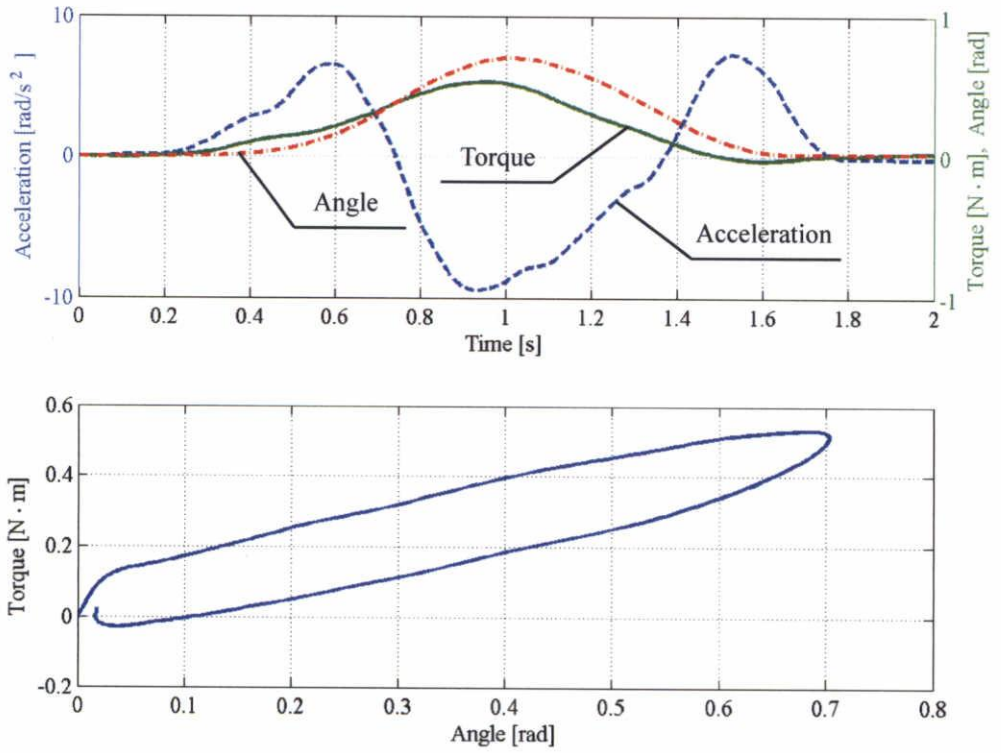


Fig. 4.18 Quick cooperative motion performed by subject D as master and subject B as slave, within 2 sec.

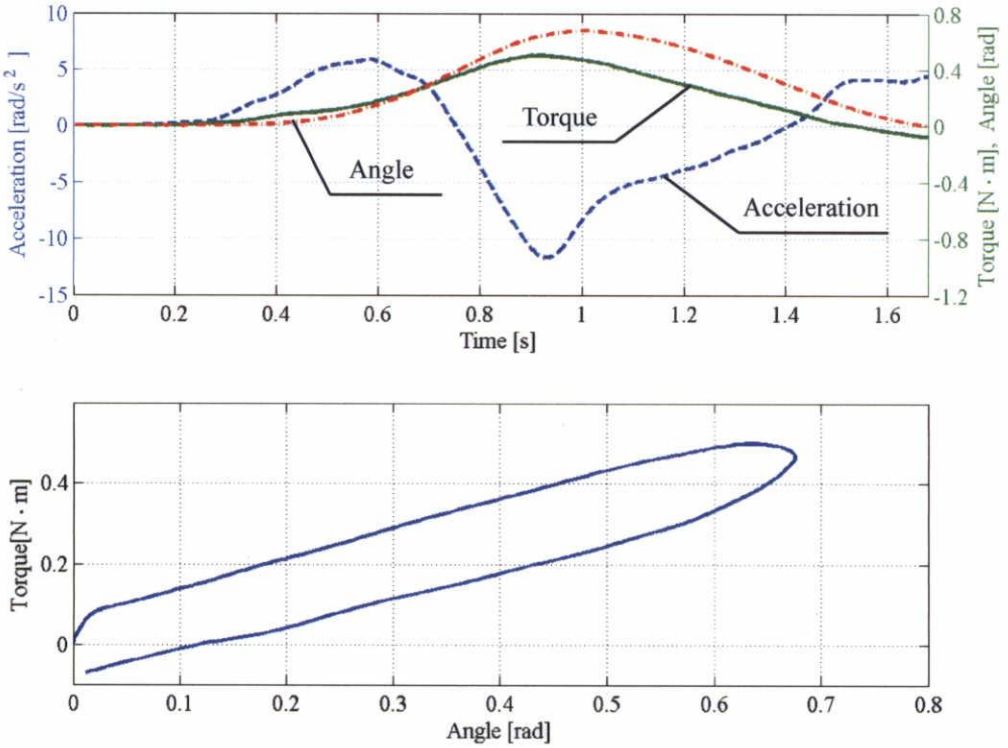


Fig. 4.19 Quick cooperative motion performed by subject E as master and subject B as slave, within 1.7 sec.

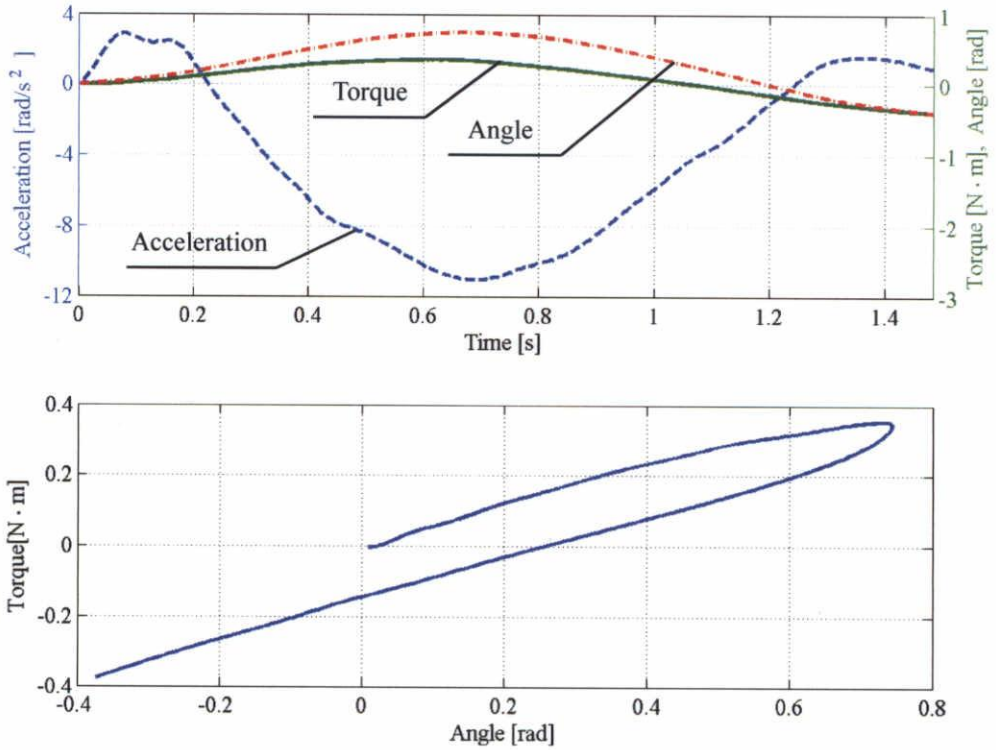


Fig. 4.20 Quick cooperative motion performed by subject G as master and subject B as slave, within 1.5 sec.

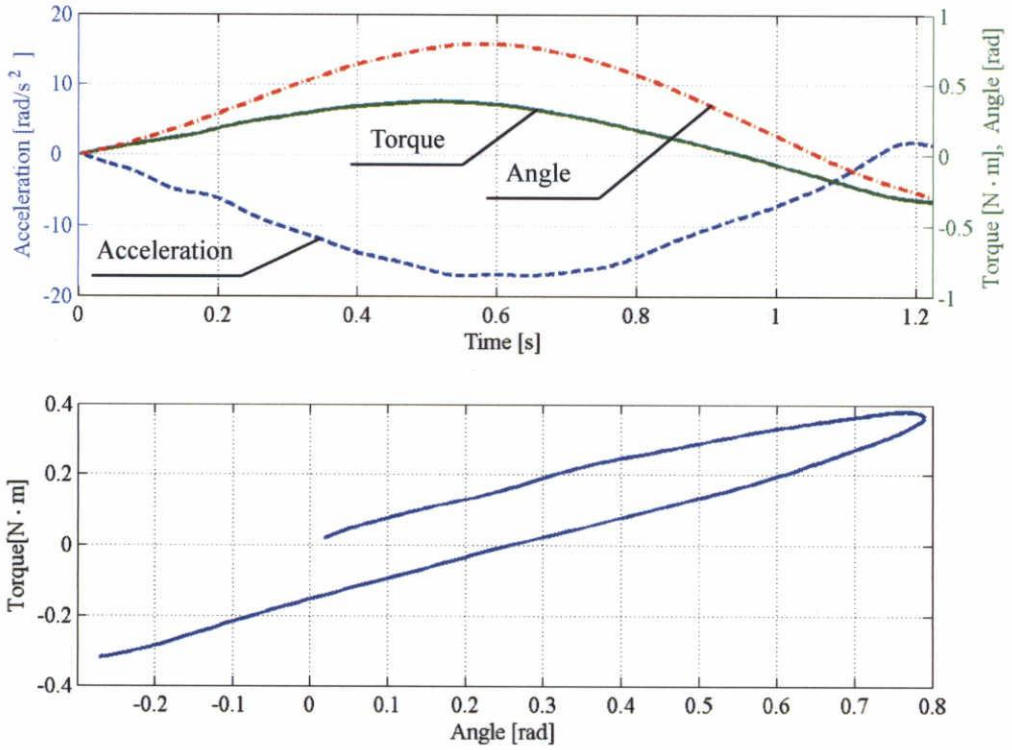


Fig. 4.21 Quick cooperative motion performed by subject H as master and subject B as slave, within 1.2 sec.

In order to verify again the characteristics of the quick cooperative motion, another uniform motion was performed. It was in CW direction only, and its velocity was about 0.7 rad/s.

The characteristics of the uniform cooperative motion are shown in Fig. 4.22 by three separate graphs. In the upper graph, the horizontal and vertical axes represent time and angular displacement, respectively. In the middle graph, the horizontal and vertical axes represent time and the torque for the slave. In the lower graph, the horizontal and vertical axes represent the angular displacement and torque for the slave. In the lower graph, the trajectory of the movement is a nearly straight line passing through the CW equilibrium position (a coordinate where the vertical coordinate value, external torque $\tau_E$ is zero).

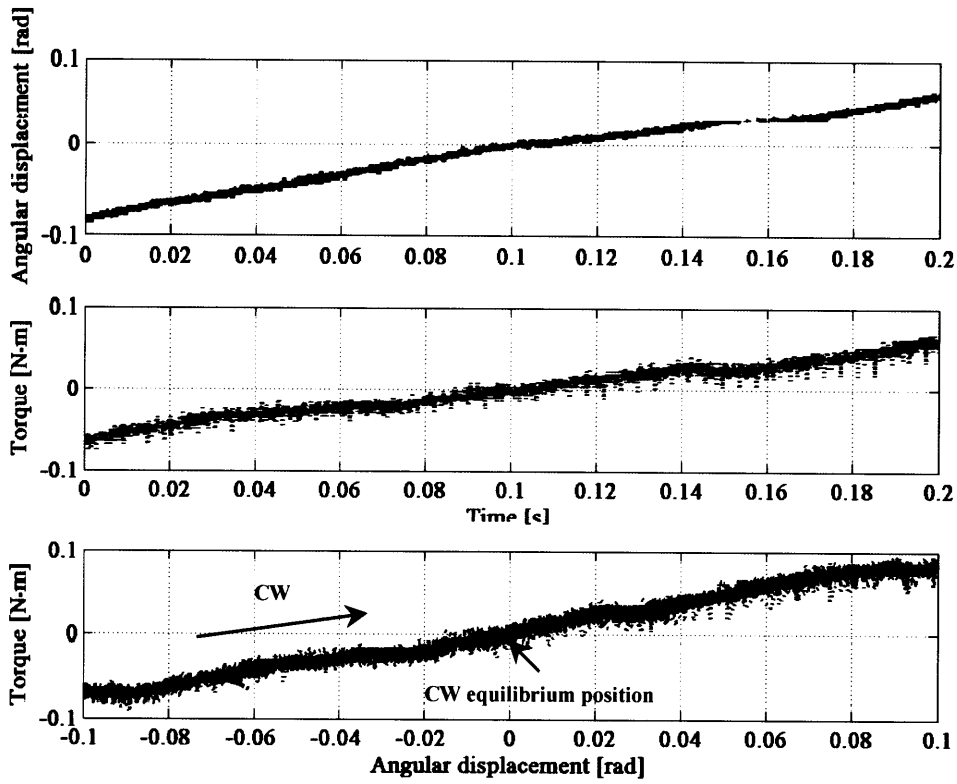


Fig. 4.22 Uniform cooperative motion performed by subject G as master and subject B as slave.

Given the slave's arm was moved to the equilibrium position in the slow cooperative motion, Eq. (7) could be expressed as:

$$K\theta + \tau_F = 0 \tag{13}$$

where the external torque $\tau_E$ was zero due to the equilibrium position, the inertia torque $I\ddot{\theta}$ and the damping torque $C\dot{\theta}$ were both zero due to the slow motion, and $u_B$ and $u_T$ were both zero due to the relaxed arm.

At the CW equilibrium position in the lower graph of Fig. 4.22, the inertia torque $I\ddot{\theta}$ is zero because of the uniform motion and $K\theta + \tau_F$ is zero from Eq. (13), and then according to Eq. (7), the damping torque $C\dot{\theta}$ is zero. In such a uniform motion, even at the equilibrium position the velocity is still around 0.7 rad/s, as a result, the damping factor $C$ must be zero. Based on this fact, the author thinks that since the damping factor $C$ is zero at the equilibrium position of such a uniform motion, it is no wonder that at other positions where the slave's arm is moved to, the damping factor $C$ is still zero.

### 4.1.3 Torque Characteristics

In the upper graph of Fig. 4.23, the horizontal axis represents time and the vertical axis represents angular velocity and angular displacement. In the middle graph, the horizontal axis represents time and the vertical axis represents the torques for both the slave and the master. In the lower graph, the horizontal and vertical axes represent the angular displacement and torque for the slave. The middle graph shows that the torque for the master increases constantly with time. Although the master

subject had to overcome the entire impedance resistance from the slave subject's arm to maintain motion, the master subject was more in control of the motion, especially during deceleration. During deceleration (after the equilibrium position), the direction of the impedance resistance was the same as the master subject's braking direction, which made it easier for the master subject to control the motion, even though he/she did not exert a braking force. In addition, the slave subject's arm provided a stable load making it easier for the master subject to slow and brake the motion. As a result, the author assumes that, in human–robot cooperative tasks, during decelerated (braking) motion, slave characteristics can be applied to a robot by means of impedance control, to make the human partner feel in better control of the motion.

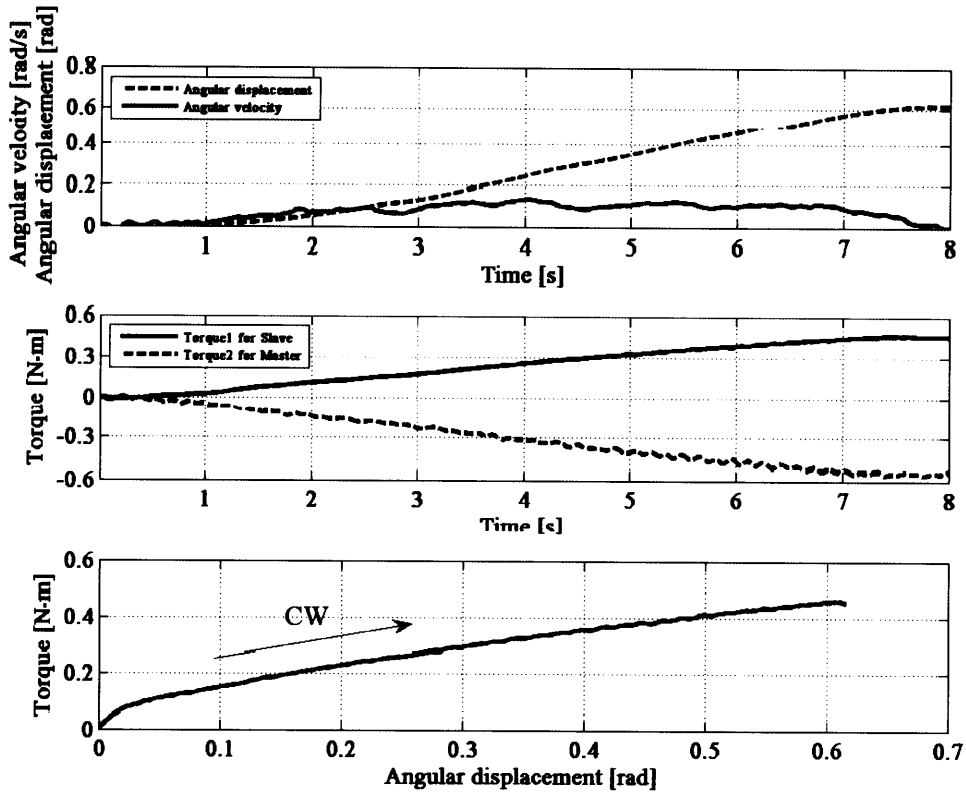


Fig. 4.23 Torque characteristics in master-slave cooperative motion, performed by subject G as master and subject D as slave.

In addition to Fig. 4.23, Figs. 4.24 to 4.29 show the torque characteristics performed by other pair combinations.

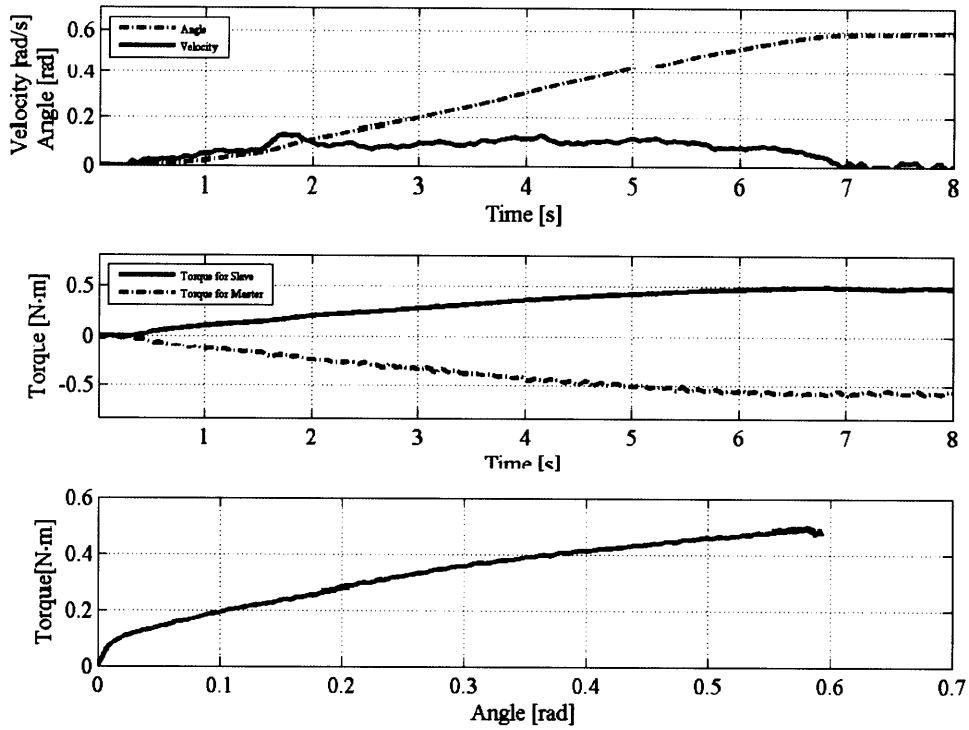


Fig. 4.24 Torque characteristics in master-slave cooperative motion, performed by subject A as master and subject D as slave.

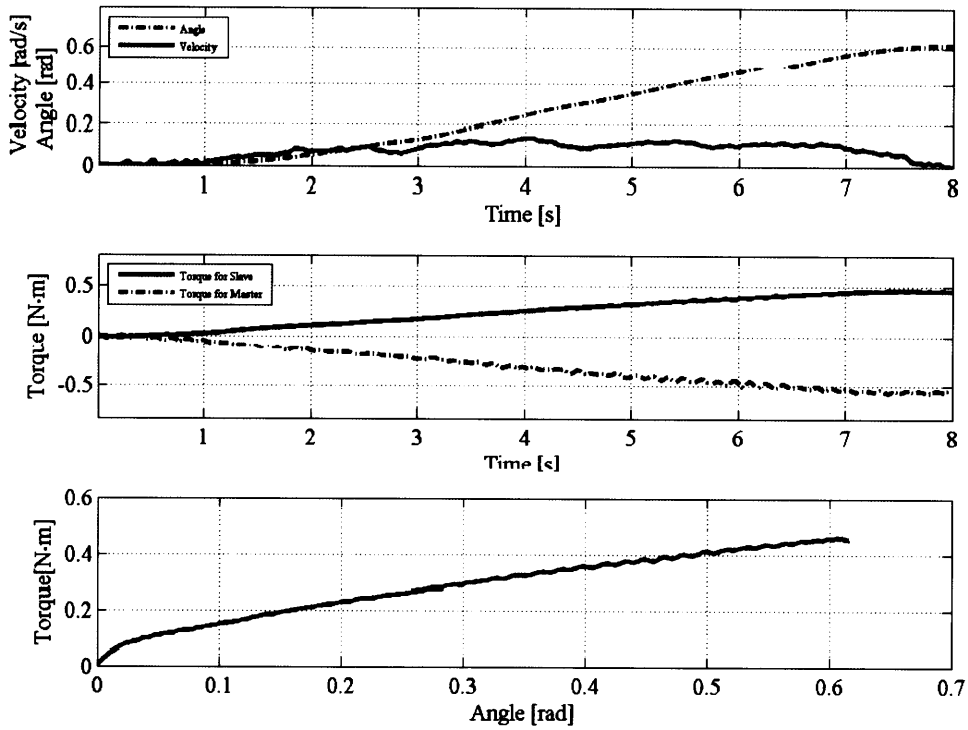


Fig. 4.25 Torque characteristics in master-slave cooperative motion, performed by subject B as master and subject D as slave.

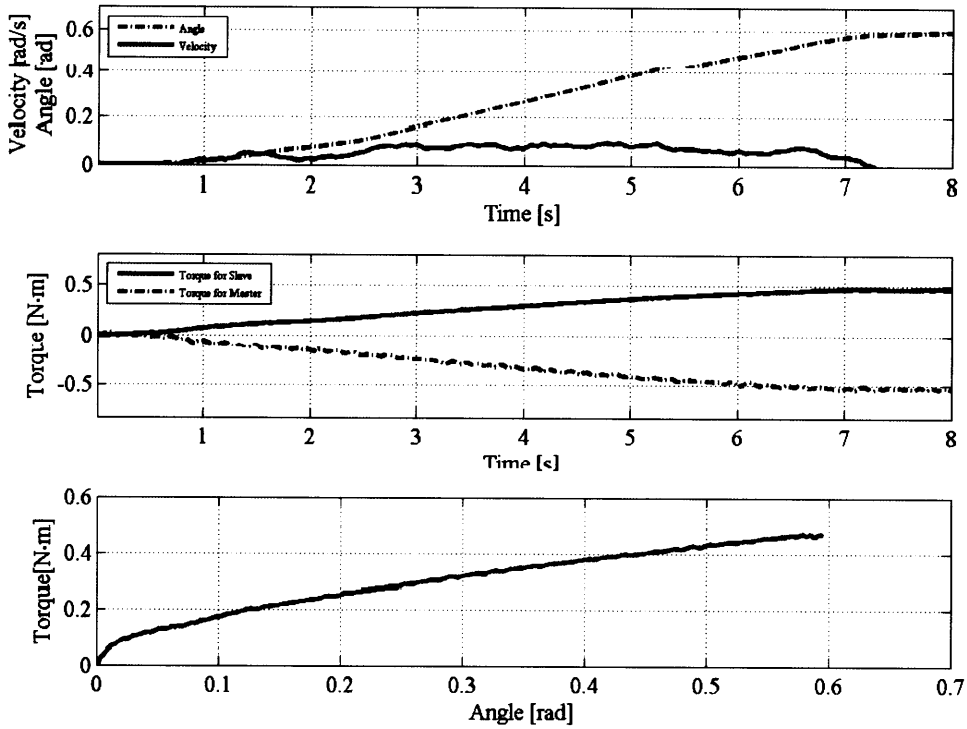


Fig. 4.26 Torque characteristics in master-slave cooperative motion, performed by subject C as master and subject D as slave.

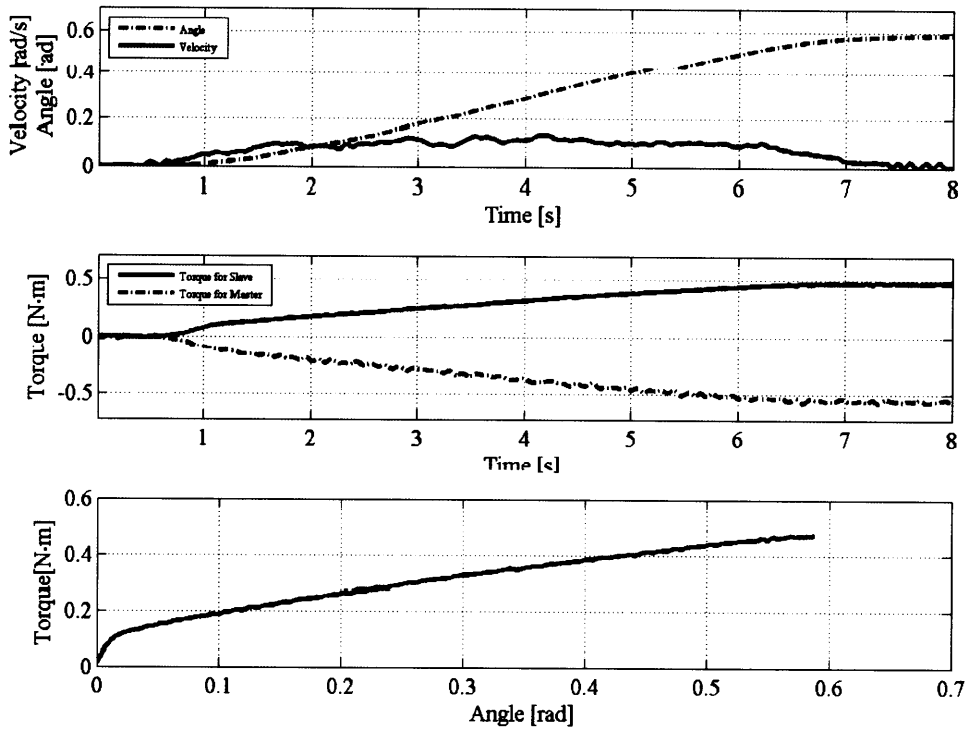


Fig. 4.27 Torque characteristics in master-slave cooperative motion, performed by subject E as master and subject D as slave.

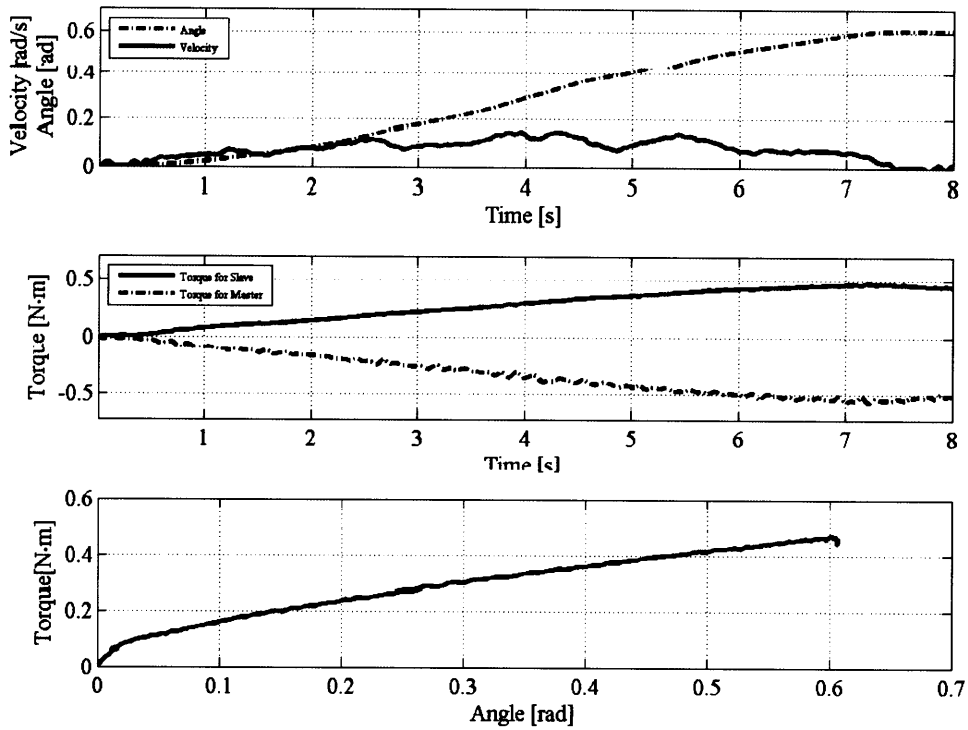


Fig. 4.28 Torque characteristics in master-slave cooperative motion, performed by subject F as master and subject D as slave.

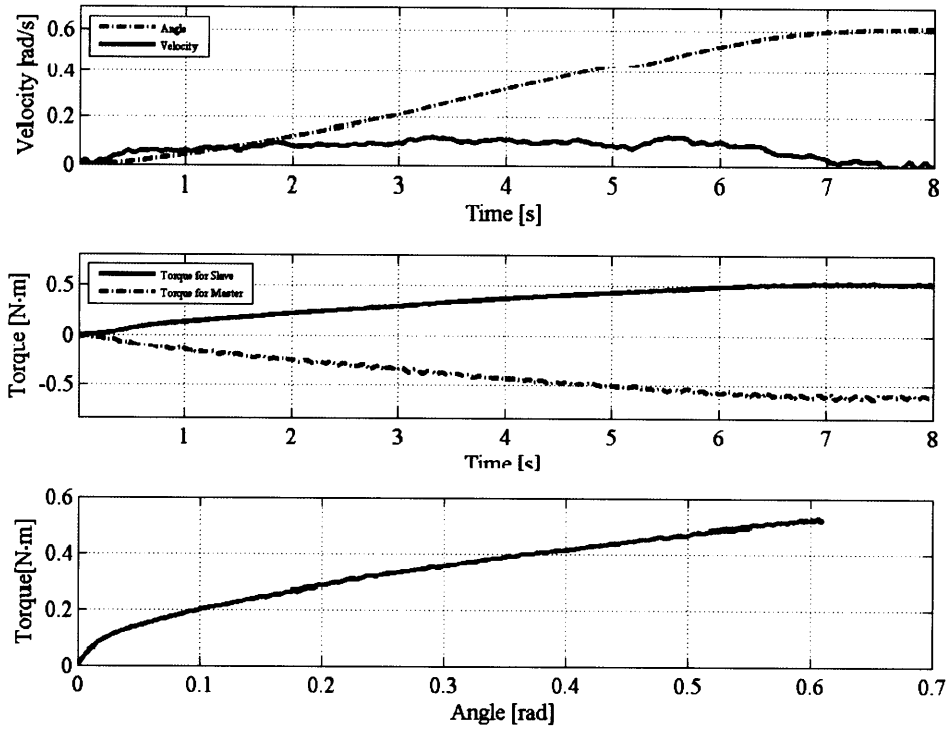


Fig. 4.29 Torque characteristics in master-slave cooperative motion, performed by subject H as master and subject D as slave.

### 4.1.4 Statistical Analysis

In this study, the author collected large amounts of experimental data from the eight subjects and found that they had common characteristics with respect to their individual parameters. Therefore, instead of showing the data for all subjects, the author shows typical sample data representative of the group.

The author used statistical analysis to demonstrate common slave characteristics—a damping factor of zero, and constant stiffness and dynamic friction. the author chose 20 sets of sample data from each pair of subjects, and obtained 320 sets of sample data from all the 16 pairs.

First, for each of the 20 sample data sets from one pair, the author used the least squares method to approximate the two curves, between −0.1 and +0.3 rad, in both CW and CCW directions, as shown in the lower graphs in Figs. 4.1 and 4.15, with two straight lines. It was thought that the two curves could be considered as straight lines if the differences between the curve and the straight line were proved to be zero. Therefore, the author performed a two-sided t test at the 0.01 significance level for the null hypothesis that the differences were zero. Consequently, the t test result (h = 0) showed that this null hypothesis could not be rejected. This verified that between −0.1 and +0.3 rad, the curves could be approximated by two straight lines. This meant that the damping factor was zero and that the stiffness was constant. Table 4.1 illustrates the average of the approximation errors for the mean and standard deviation (SD) for all the 320 sets of sample data.

Table 4.1 Statistical analysis of stiffness characteristics in master-slave cooperative motion.

| Direction | Mean of approximation errors | SD of approximation errors |
|---|---|---|
| CW | 0.0056 | 0.0077 |
| CCW | 0.0064 | 0.0091 |

Next, for each of the 20 sets of sample data from one pair, the author calculated the mean $H$ values between −0.1 and +0.3 rad, as shown in the lower graphs of Figs. 4.1 and 4.15. It was thought that the value of $H$ would be constant if the differences between the $H$ values and the mean of $H$ values were proved to be zero. Therefore, the author performed a two-sided t test at the 0.01 significance level for the null hypothesis that the differences were zero. Consequently, the t test result (h = 0) showed that this null hypothesis could not be rejected. This verified that the value of $H$ between −0.1 and +0.3 rad was constant; thus implying that the dynamic friction was constant. Table 4.2 illustrates the average of the differences for the mean and the SD for all the 320 sets of sample data.

Table 4.2 Statistical analysis of dynamic friction characteristics in master-slave cooperative motion.

| Means of differences | SD of differences |
|---|---|
| 0.0109 | 0.0165 |

# CHAPTER 5

# MASTER-MASTER COOPERATIVE EXPERIMENTS

## 5.1 Master–Master Cooperative Motion

### 5.1.1 Method

The following experiment was designed to find the cooperative characteristics in master–master cooperative motion. To perform master–master cooperative motion, both subjects in each pair played a master, simultaneously (i.e., performing active arm movements). The author discovered that as long as one subject started the motion a little bit later than the other, they exhibited master–slave cooperation instead of master–master cooperation. Since the time of the cooperative motion was short (only 8 sec), once the subjects started master–slave cooperation, there was no time for them to switch to master–master cooperation. As a result, rather than instructing one subject to act as the master at the beginning of the motion, the author instructed this subject to act as a slave from the start to the end of the accelerated motion, and then rotate the load cooperatively with the other subject to the end of the motion. In other words, in the initial part of the motion, the subject performed passive (slave) movements, then switched to active arm movement as a master from

the halfway of the motion.

Because this subject played the role of the master just for a portion of the motion, the author called this role a semi-master. In master–master cooperative motion, the subject who is the master from the beginning tracked the position by watching the display monitor throughout the motion, and the semi-master watched it from the halfway point of the motion.

### 5.1.2 Experimental Result

The torques for both the semi-master and the master, shown in Fig. 5.1, were measured for comparison with those for master–slave cooperative motion (Fig. 4.23). The torques in the middle graph of Fig. 5.1 show that during the master–master cooperation, the two subjects' torques decreased to a certain level and then remained almost constant. The lower graph shows the relation between the torque and the angular displacement for the semi-master. When master–slave cooperation switched to master–master cooperation, for the semi-master, the stiffness characteristics shown in the passive arm movement disappeared, and the torque shown in the active arm movement maintained the same value as it had in the last moment of passive arm movement. That was because the semi-master subject had to exert active strength to perform cooperative motion with the master subject, and the arms of both subjects could be considered as actuators—it was unnecessary for them to move each other's arms by exerting extra strength. Therefore, in master–master cooperative motion, the master subject felt it easier to perform active arm movement than during the master–

slave cooperative motion. When the author changed the weight of the load during the experiment in master–master cooperative motion, the torques for the two subjects stayed constant at different levels; however, the cooperative characteristics were unchanged.

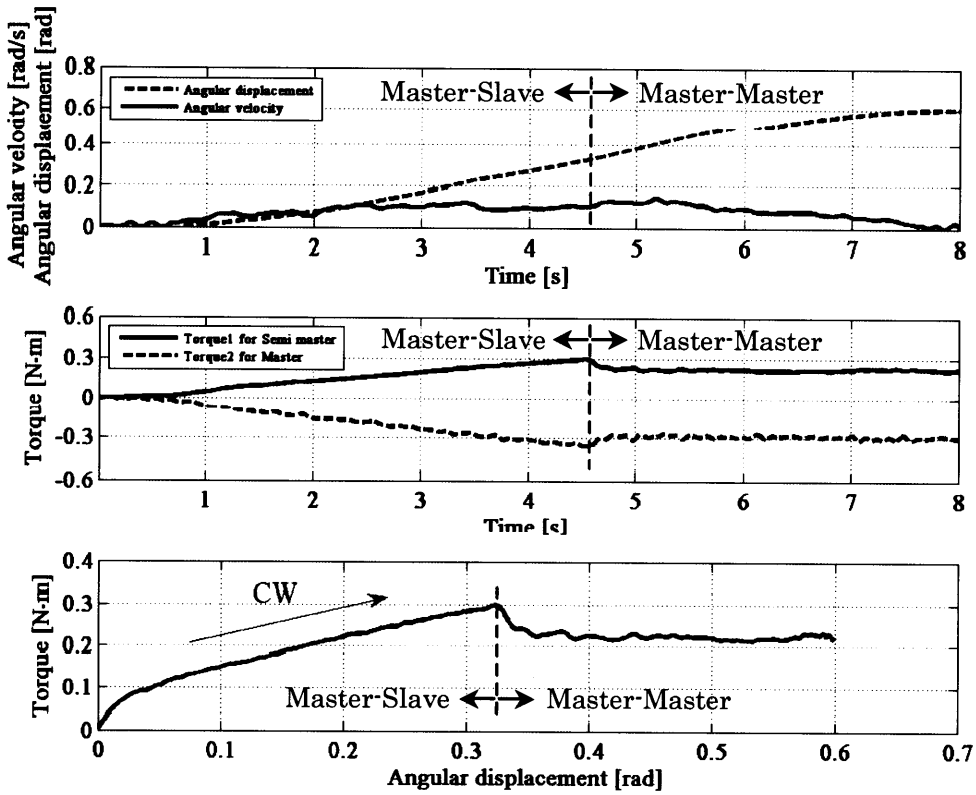


Fig. 5.1 Torque characteristics in master–master cooperative motion, performed by subject H as master and subject E as semi-master.

In addition to Fig. 5.1, Figs. 5.2 to 5.7 show the torque characteristics performed by other pair combinations.

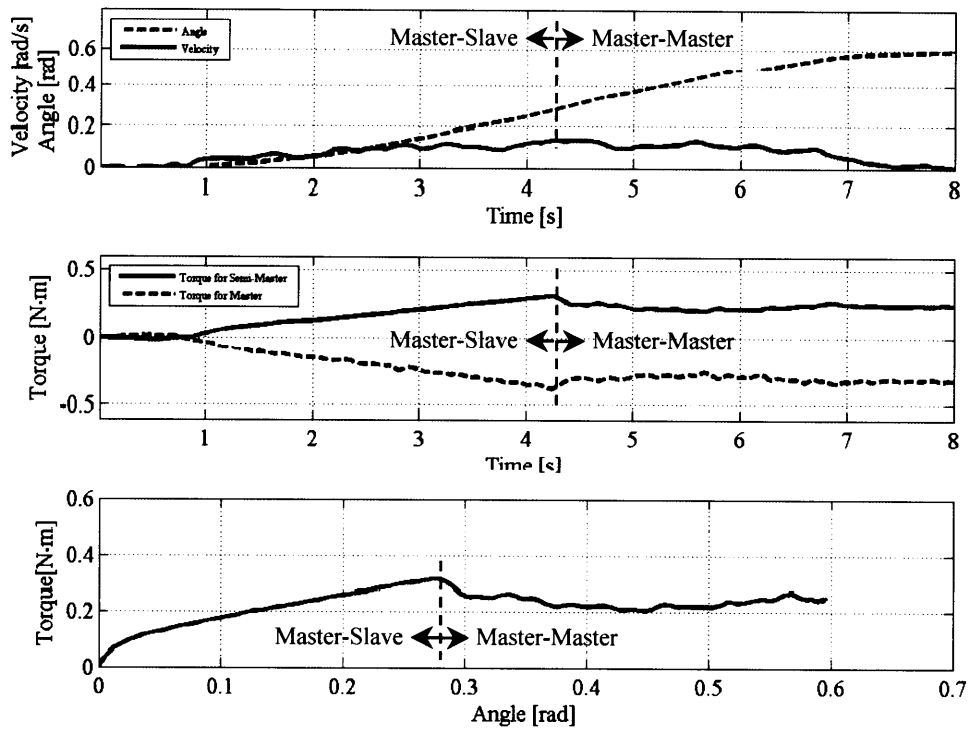


Fig. 5.2 Torque characteristics in master–master cooperative motion, performed by subject A as master and subject E as semi-master.

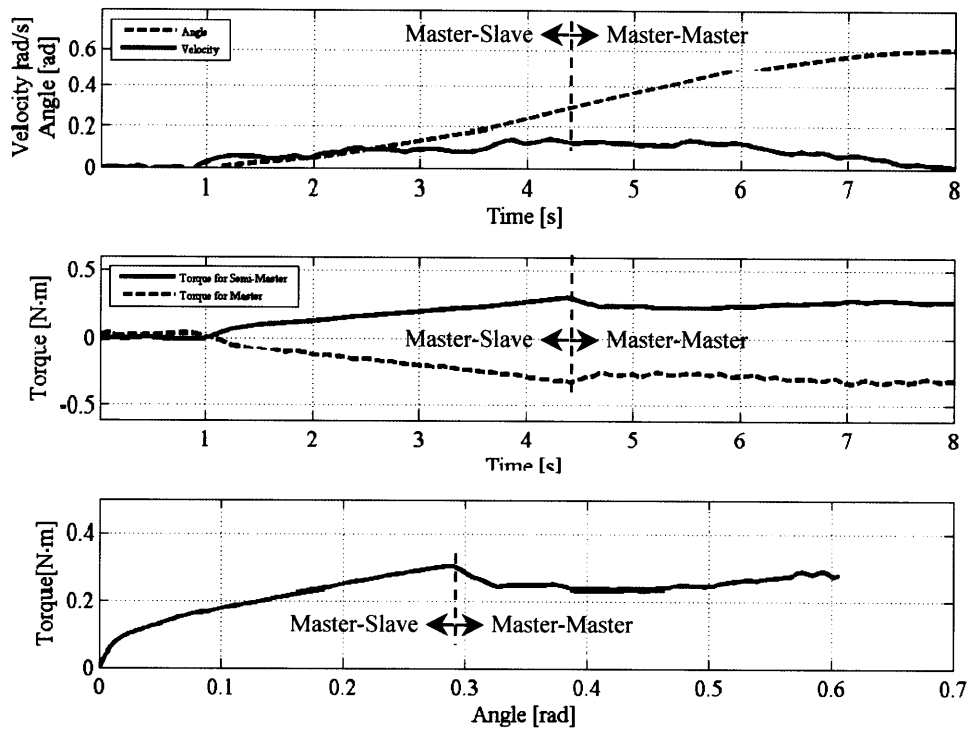


Fig. 5.3 Torque characteristics in master–master cooperative motion, performed by subject B as master and subject E as semi-master.

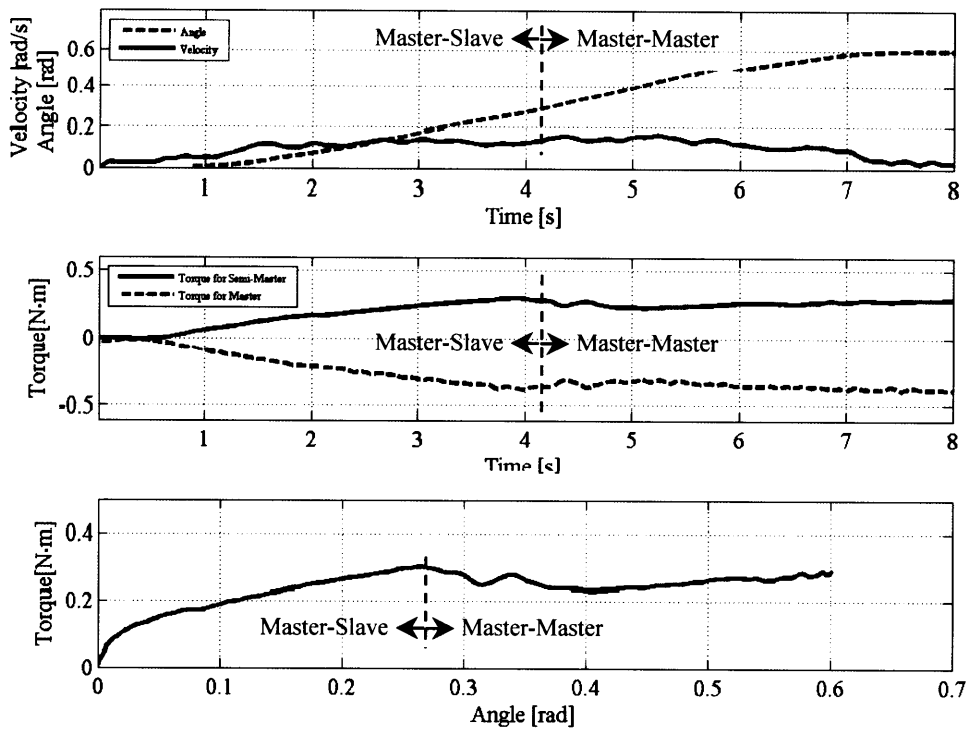


Fig. 5.4 Torque characteristics in master–master cooperative motion, performed by subject C as master and subject E as semi-master.

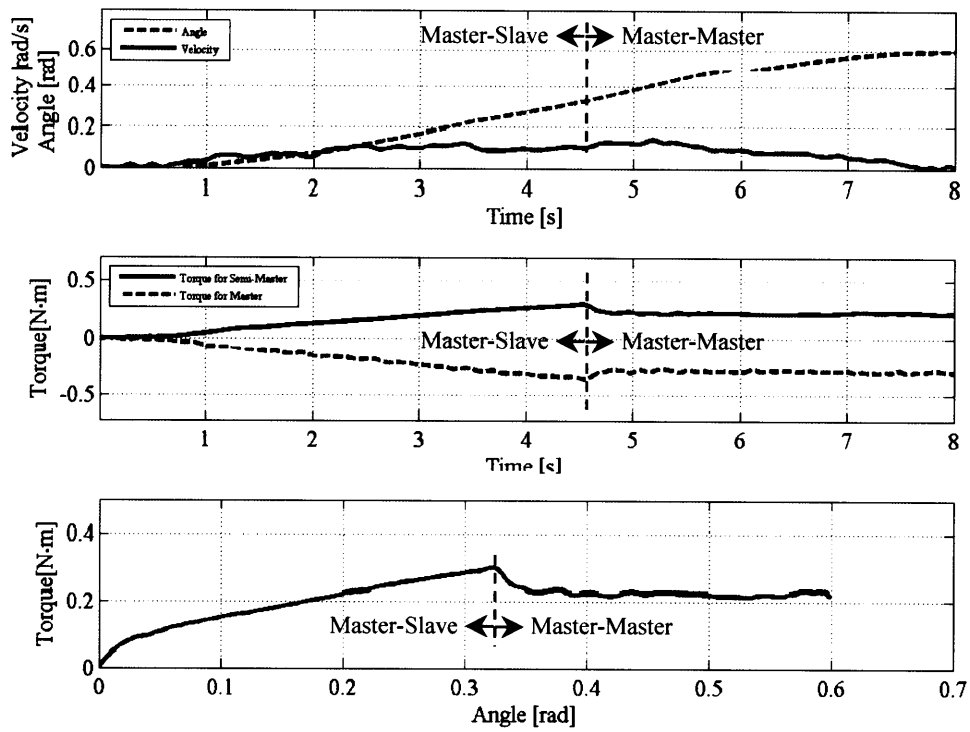


Fig. 5.5 Torque characteristics in master–master cooperative motion, performed by subject D as master and subject E as semi-master.

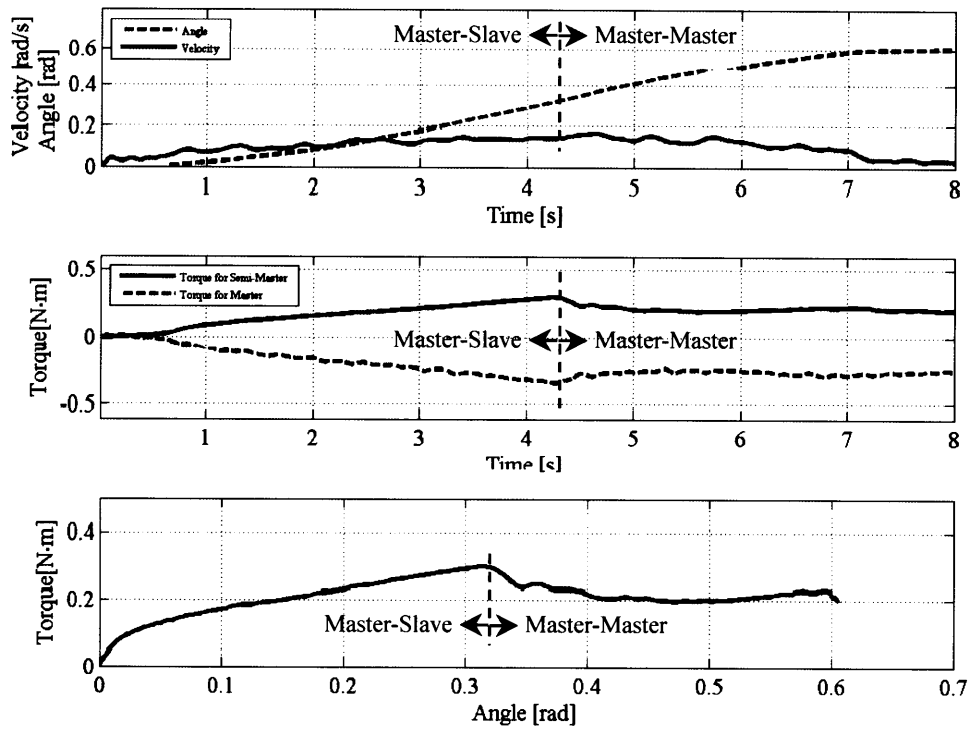


Fig. 5.6 Torque characteristics in master–master cooperative motion, performed by subject F as master and subject E as semi-master.

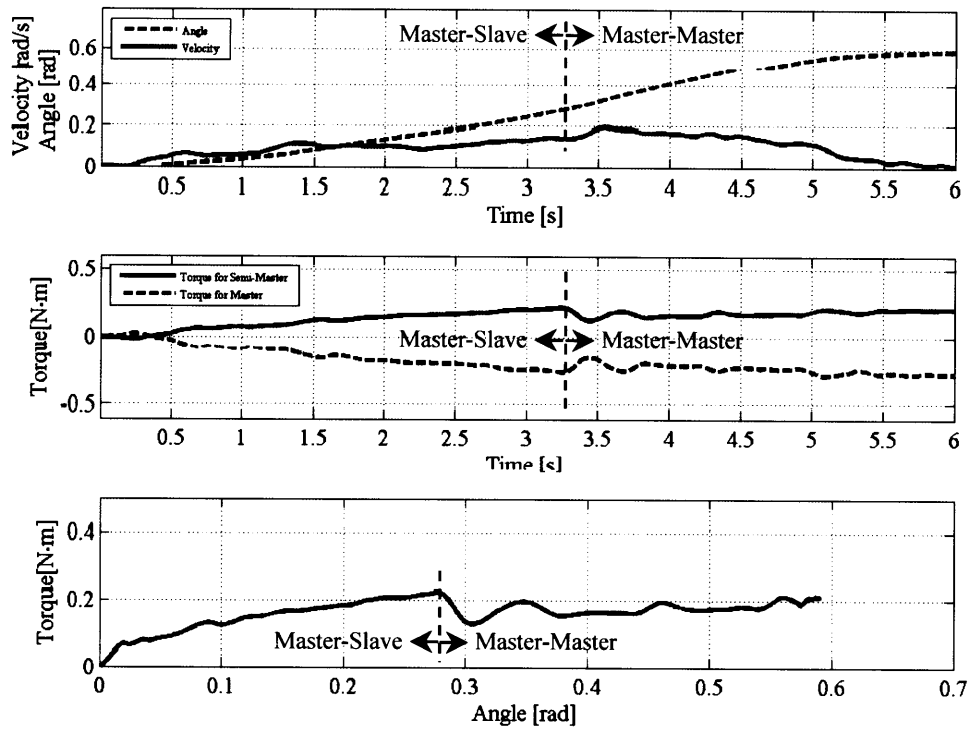


Fig. 5.7 Torque characteristics in master–master cooperative motion, performed by subject G as master and subject E as semi-master.

### 5.1.3 Statistical Analysis and Discussion

The author performed a statistical analysis to demonstrate the common characteristics of the semi-master—the constant torque. For each of the 20 sample data sets from one pair, the author used least squares to approximate the curve between 0.35 and 0.6 rad, as shown in the lower graph of Fig. 5.1, with a horizontal straight line. The curve could be considered as a horizontal straight line if the differences between the curve and the horizontal straight line were proved to be zero. Therefore, the author performed a two-sided t test at the 0.01 significance level for the null hypothesis that the differences were zero. Consequently, the t test result (h = 0) showed that this null hypothesis could not be rejected. This verified that the curve between 0.35 and 0.6 rad could be approximated by a horizontal straight line, which meant that the torque was constant. Table 5.1 illustrates the average of the approximation errors for the mean, and the SD for all the 320 sets of sample data.

Table 5.1 Statistical analysis of torque characteristics in master–master cooperative motion.

| Mean of approximation errors | SD of approximation errors |
|---|---|
| 0.0126 | 0.0183 |

Thus, the author assumes that in human–robot cooperative tasks, torque control can be used during accelerated motion, with compensation for the weight of the load between the human and the robot, as well as for the force exerted by the human in applying the characteristics of the semi-master to a robot. In this case, some type of power assist robot can lighten the burden on its human partner in performing cooperative tasks.

# CHAPTER 6

# CONCLUSIONS

In this study, the author analyzed the characteristics of the human arm in master–slave and master–master cooperative motions, using a single rotational degree-of-freedom experimental system.

The author found that the slave's arm could be represented with a mass-spring-friction biomechanical model, in which the damping factor was zero, and the stiffness and dynamic friction were both individually constant within the investigated range. To ensure the usefulness of the parameters or estimated characteristics for real applications, the author examined the study by Rahman *et al.* who determined the impedance characteristics of the human arm and implemented estimated parameters for robot control in a cooperative task with a human[21]. The implementation result convinced the author that the human arm characteristics that Rahman *et al.* found could be applied to the control of a cooperative robot working with a human. Therefore, the author assumes that implementing the human arm characteristics found in this study into human–robot cooperative tasks (taking advantage of the experimental method that Rahman *et al.* proposed) should achieve better cooperative characteristics.

The analysis of torque characteristics in maser–slave and master–master cooperative motions revealed that in master–slave cooperative motion, the master subject felt it easier to control the motion, especially during deceleration, and in master–master cooperative motion, the master subject felt it easier to perform the active arm movement than in master–slave cooperative motion. As a result, in human–robot cooperative tasks, during accelerated motion the characteristics of the semi-master can be applied to a robot by using torque control. The robot can provide power assistance in compensating for the weight of the load that the human and the robot both bear; the human then needs to exert less force to accelerate the motion. During decelerated (braking) motion, the characteristics of the slave can be applied to a robot by impedance control, and the robot can make it easier for the human to control the motion.

# REFERENCES


(1) http://www.faculty.ucr.edu/~currie/roboadam.htm

(2) http://en.wikipedia.org/wiki/Robot

(3) Nakano, E., Ozaki, S., Ishida, T., and Kato, I., Co-operational control of the anthropomorphous manipulator 'MELARM', *Proceedings of 4th International Symposium on International Robots*, (1974), pp. 251-260.

(4) Zheng, Y.F., and Luh, J.Y.S., Optimal load distribution for two industrial robots handling a single object, *Proceedings of IEEE International Conference on Robotics and Automation*, (1988), pp. 344-349.

(5) Pittelkau, M.E., Adaptive load-sharing force control for two-arm manipulators, *Proceedings of IEEE International Conference on Robotics and Automation*, (1988), pp. 498-503.

(6) Kopf, C.D., and Yabuta, T., Experimental comparison of master/slave and hubrid two arm position/force control, *Proceedings of IEEE International Conference on Robotics and Automation*, (1988), pp. 1633-1637.

(7) Al-Jarrah, O.M., and Zheng, Y.F., Arm-manipulator coordination for load sharing using variable compliance control, *Proceedings of IEEE International Conference on Robotics and Automation*, (1997), pp. 895-900.

(8) kosuge, K., and Kazamura, N., Control of a robot handling an object in cooperation with a human, *Proceedings of IEEE International Workshop on Robot and Human Communication*, (1997), pp. 142-147.

(9) Ikeura, R., and Inooka, H., Variable impedance control of a robot for cooperation with a human, *Proceedings of IEEE International Conference on Robotics and Automation*, Vol. 3 (1995), pp. 3097-3102.

(10) Ikeura, R., Morita, A., and Mizutani, K., Variable damping characteristics in carrying an object by two humans, *Proceedings of IEEE International Workshop on Robot and Human Communication*, (1997), pp. 130-134.

(11) Ikeura, R., Kozawa, H., and Mizutani, K., Variable damping control for a robot cooperating with a human in carrying an object and its experimental evaluation, *Proceedings of the Japan–USA Symposium on Flexible Automation*, (1998), pp. 29-34.

(12) Ikeura, R., Moriguchi, T., and Mizutani, K., Optimal variable damping control for a robot carrying an object with a huamn, *Proceedings of international Conference on Control, Automation and Systems*, (2001), pp. 63-66.

(13) Ikeura, R., Inooka, H., and Mizutani, K., A control method for a robot cooperating with a human in carrying an object, *Proceedings of the Japan–USA Symposium on Flexible Automation*, (1996), pp. 255-260.

(14) Ikeura, R., and Mizutani, K., Control of robot cooperating with human motion, *Proceedings of 7th IEEE International Workshop on Robot and Human Communication*, (1998), pp. 525-529.

(15) Ikeura, R., Monden, H., and Inooka, H., Cooperative motion control of a robot and a human, *Proceedings of IEEE International Workshop on Robot and Human Communication*, (1994), pp. 112-117.

(16) Ikeura, R., and Inooka, H., Cooperative force control in carrying an object by two humans, *Proceedings of IEEE International Conference on Systems, Man, and Cybernetics*, (1995), pp. 2307-2311.

(17) Ikeura, R., Inooka, H., and Mizutani, K., Subjective evaluation for maneuverability of a robot cooperating with humans, *Journal of Robotics and Mechatronics*, Vol. 14, No. 5 (1999), pp. 324-329.

(18) Rahman, M.M., Ikeura, R., and Mizutani, K., Analysis of cooperation characteristics of two humans in moving an object, *Proceedings of the International Conference on Mechatronics and Information Technology*, (2001), pp. 454-458.

(19) Rahman, M.M., Ikeura, R., and Mizutani, K., Control characteristics of two humans in cooperative task, *Proceedings of IEEE International Conference on Systems, Man and Cybernetics*, (2000), pp. 1301-1306.

(20) Rahman, M.M., Ikeura, R., and Mizutani, K., Cooperation characteristics of two humans in moving an object, *Machine Intelligence and Robotic Control*, Vol. 4, No. 2 (2002), pp. 43-48.

(21) Rahman, M.M., Ikeura, R., and Mizutani, K., Control characteristics of two humans in cooperative task and its application to robot control, *Proceedings of IEEE International Conference on Industrial Electronics, Control and Instrumentation*, Vol. 3 (2000), pp. 1773-1778.

(22) Rahman, M.M., Ikeura, R., and Mizutani, K., Investigation of the impedance characteristic of human arm for development of robots to cooperate with humans, *JSME International Journal*, Series C, Vol. 45, No. 2 (2002), pp. 510-518.

(23) Rahman, M.M., Ikeura, R., and Mizutani, K., Impedance characteristics of human arm for cooperative robot, *Proceedings of the International Conference on Control Automation and Systems*, (2002), pp. 1455-1460.

(24) Engin, A.E., On the biomechanics of the shoulder complex, *Journal of Biomechanics*, Vol. 13 (1980), pp. 575-590.

(25) Gomi, H., Koike, Y., and Kawato, M., Human hand stiffness during discrete point-to-point multi-joint movement, *Proceedings of the Annual International Conference of the IEEE Engineering in Medicine and Biology Society*, Vol. 4 (1992), pp. 1628-1629.

(26) Gomi, H., and Osu, R., Task-dependent viscoelasticity of human multi-joint arm and its spatial characteristics for interaction with environments, *Journal of Neuroscience*, Vol. 18, No. 21 (1998), pp. 8965-8978.

(27) Maurel, W., and Thalmann, D., A case study on human upper limb modeling for dynamic simulation, *Computer Methods in Biomechanics and Biomedical Engineering*, Vol. 2, No. 1 (1999), pp. 65-82.

(28) Maurel, W., Thalmann, D., Hoffmeyer, P., Beylot, P., Gingins, P., Kalra, P., and Magnenat Thalmann, N., A biomechanical musculoskeletal model of human upper limb for dynamic simulation, *Proceedings of the Eurographics Workshop on Computer Animation and Simulation*, (1996), pp. 121-136.

(29) Cannon, S.C., and Zahalak, G.I., The mechanical behavior of active human skeletal muscles in small oscillations, *Journal of Biomechanics*, Vol. 15, No. 2 (1982), pp. 111-121.

(30) http://en.wikipedia.org/wiki/Upper_limb

(31) http://en.wikipedia.org/wiki/Shoulder

(32) http://en.wikipedia.org/wiki/Arm

(33) http:// physicaltherapy.about.com/od/humananatomy.html

(34) http://en.wikipedia.org/wiki/Elbow-joint

(35) Bizzi, E., Hogan, N., Mussa-Ivaldi, F.A., and Giszter, S., Does the nervous system use equilibrium-point control to guide single and multiple joint

movements, *Behavioral and Brain Sciences*, Vol. 15, No. 4 (1992), pp. 603-613.

(36) Shadmehr, R., Control of equilibrium position and stiffness through postural modules, *Journal of Motor Behavior*, Vol. 25, No. 3 (1993), pp. 228-241.

(37) Gomi, H., and Kawato, M., Equilibrium-point control hypothesis examined by measured arm stiffness during multi-joint movement, *Science*, Vol. 272 (1996), pp. 117-120.

(38) Ljung, L., System Identification Toolbox, User's Guide, USA, *The MathWorks Inc.*, Commands and Functions (1995).